
Design of a Fuel-Efficient Guidance System for a STOL Aircraft

John D. McLean and Heinz Erzberger

March 1981



National Aeronautics and
Space Administration

TABLE OF CONTENTS

	<u>Page</u>
SYMBOLS	iii
SUMMARY	1
INTRODUCTION	1
ENERGY-RATE MODEL	3
SELECTION OF REFERENCE CONTROLS	5
TRAJECTORY SYNTHESIS	7
Synthesis of Horizontal Paths	8
Synthesis of Speed-Altitude Profiles	8
Lead Distances	13
Temperature Compensation	13
Temperature Profile Estimation	14
Wind Profile Estimation	14
Computation Time	14
REAL-TIME TRAJECTORY GENERATION (TRACK MODE).	15
PERTURBATION CONTROL LAW	16
STRUCTURE AND OPERATION OF THE FLIGHT SYSTEM	18
CONCLUDING REMARKS	20
APPENDIX — AIRBORNE COMPUTER IMPLEMENTATION	21
REFERENCES	33
TABLES	34
FIGURES	42

SYMBOLS

D	drag force, lb
E	energy, ft
\dot{E}_n	normalized energy rate, nondimensional
$\dot{E}_{n\max}, \dot{E}_{n\min}$	maximum and minimum available normalized energy rate, respectively
F, G	perturbation state and control distribution matrices, respectively
g	acceleration of gravity, ft/sec
H_f, H_i	final and initial ground heading of aircraft, respectively, deg
h	altitude, ft
h_f, h_i	final and initial altitudes of aircraft, respectively, ft
K	feedback gain matrix
$k_{\phi_y}, k_{\dot{\phi}_y}$	lateral error and error-rate feedback gains
L	lift force, lb
m	aircraft mass, slugs
S	distance along ground track
\dot{S}	speed along ground track, ft/sec
S_b, S_f	distance of backward and forward integration, respectively
S_c	cruise distance, ft
S_h	length of ground track from initial to final position of aircraft, ft
T	thrust, lb
t	time, sec
u	perturbation control vector
V_a	true airspeed, ft/sec or knots

V_{EQ}	equivalent airspeed, ft/sec or knots
V_f, V_i	final and initial airspeeds of aircraft, respectively, ft/sec or knots
V_{GR}	reference groundspeed, ft/sec
V_{TA}	nominal V_{EQ} for terminal area
V_w	wind speed, knots
V_{wat}	component of wind along reference horizontal track
W	(aircraft weight)/ $\cos \phi$, lb
X_f, X_i	final and initial x coordinates of aircraft, respectively, ft
x	perturbation state vector
Y_f, Y_i	final and initial y coordinates of aircraft, respectively, ft
y	crosstrack error, ft
\dot{y}	crosstrack error rate, ft/sec
α	angle of attack, deg
γ_A	aerodynamic flightpath angle, rad or deg
γ_I	inertial flightpath angle, deg
δ_f	flap angle, deg
$\delta_{f_{max}}$	maximum flap angle, deg
ϵ	fraction of energy rate used for changing speed
θ_c	command pitch angle, deg
ν	vectored thrust, in degrees of nozzle angle
π	power setting, in percent
σ	fraction of available energy rate
ϕ	bank angle, deg
ϕ_c, ϕ_r	commanded and reference bank angles, respectively, deg

DESIGN OF A FUEL-EFFICIENT GUIDANCE SYSTEM FOR A STOL AIRCRAFT

John D. McLean and Heinz Erzberger

Ames Research Center

SUMMARY

A fuel-conservative guidance system for powered-lift STOL aircraft operating in terminal areas has been developed and evaluated in flight. In the predictive mode, the system synthesizes a horizontal path from an initial aircraft position and heading to a desired final position and heading and then synthesizes a fuel-efficient speed-altitude profile along the path. In the track mode, the synthesized trajectory is reconstructed and tracked automatically. This paper presents the analytical basis for the design of the system and a description of the airborne computer implementation. A detailed discussion of the software, which should be helpful to those who use the actual software developed for these tests, is also provided.

INTRODUCTION

In the past, terminal-area guidance system design for aircraft has concentrated primarily on automatic glide-slope tracking, flare, and touchdown. During recent years, designs have been developed to provide automatic guidance along curved and decelerating approach paths. This increased capability was made possible through the integration of digital computers into the flight guidance system. However, even in the more advanced designs, automatic guidance is limited to a few prestored three-dimensional flightpaths. Although the ability to fly complex prestored trajectories is essential, it cannot give optimum performance under actual terminal-area operating conditions, as shall be explained.

First, a prestored trajectory can optimize neither fuel consumption nor certain other performance measures under actual operating conditions. Optimum trajectories depend significantly on aircraft gross weight, wind and temperature profiles, and on the type of constraints imposed. These variables cannot be predicted reliably prior to takeoff. To prestore optimum trajectories for each combination of variables likely to be encountered would result in an impossibly large memory requirement. Therefore, prestored trajectories must necessarily represent a compromise in performance.

Second, in existing systems the pilot must fly the aircraft manually from some initial position to the starting point of the prestored or fixed trajectory. Flight along this segment is known as the capturing maneuver. Three-dimensional, curved trajectories can be difficult to capture manually, and, if the trajectory also includes a specification of landing time, as is the case in four-dimensional (4D) guidance, the capturing maneuver cannot be done by

the pilot without computer assistance. Therefore, the capturing maneuver, because of its variability, can only be generated by onboard trajectory synthesis.

Third, aircraft entering high-density airspace for a landing approach are usually controlled by air traffic control vectors, and during this period they are often forced to deviate from a prestored flightpath. Resumption of flight on a prestored path can only begin after the aircraft has received its final vector, clearing it for approach. But the initial position of the aircraft at that time is a variable, thus requiring a capturing maneuver and, therefore, onboard synthesis.

With the onboard trajectory synthesis algorithm presented in this paper, an onboard computer rapidly calculates an efficient and flyable aircraft trajectory that meets specified initial and final conditions and that is subject to various constraints. If a portion of the trajectory, such as the final approach, is fixed, the algorithm generates the desired airspeed and flight-path angles along the fixed segments. If the trajectory is not fixed, the algorithm will synthesize the trajectory both horizontally and vertically, based on the minimum-fuel or minimum-noise criterion. The latter trajectory synthesis is often required to capture a prestored or fixed trajectory and is therefore called the capture mode.

An initial design of a four-dimensional guidance system embodying the concept of onboard trajectory synthesis, including the capture mode, was developed and flight tested on board a Convair 340 aircraft equipped with STOLAND avionics (ref. 1). In the design described here a similar approach is used in that the synthesis problem is separated into two parts: the synthesis of the horizontal trajectory and the generation of speed and altitude profiles compatible with the horizontal path. However, an improved algorithm was used for synthesis of the horizontal track (developed in ref. 2), and vertical and speed profiles are synthesized by a more sophisticated method using simplified aero-propulsion performance models of the aircraft (ref. 3). This results in profiles that are more nearly optimum in terms of fuel conservation. Design of the control law for tracking the synthesized trajectory is based on a linearized perturbation guidance approach. Since the perturbation equations are aircraft-configuration-dependent, gain scheduling is used in the feedback law.

The Augmentor Wing Jet STOL Research Aircraft (AWJSRA) was chosen as the test vehicle for this concept. This type of powered-lift aircraft is not only highly cost-sensitive to operational procedures in the terminal area, but also exemplifies particularly well the unique problems of powered-lift aircraft. Those problems are high fuel consumption in the STOL mode, dependence of both lift and drag on thrust, and an excess of controls over the minimum number needed to determine path and speed. These factors suggest that trajectory optimization could greatly increase the operational efficiency of the aircraft. Implementation of this concept was facilitated by the existing installation of the STOLAND avionics system on board the aircraft.

This paper presents the analytical basis for the system and a description of the computer implementation. The implementation was done initially in FORTRAN and was run on a large general-purpose computer (ref. 4); it was then evaluated in a piloted simulation and in flight. The description of the computer implementation is presented in abbreviated form in the appendix; nevertheless, the information provided there should be sufficient to permit application of the techniques to other aircraft.

ENERGY-RATE MODEL

An energy-rate model of aircraft performance has been found to yield a compact and sufficiently accurate representation of performance for terminal-area trajectory synthesis. In this section a performance model based on energy rate is derived following the approach used in reference 5. The energy E is defined by

$$E = h + \frac{1}{2g} (V_a^2) \quad (1)$$

Differentiation of equation (1) with respect to time gives

$$\dot{E} = \dot{h} + \frac{V_a \dot{V}_a}{g} \quad (2)$$

The airspeed V_a is the magnitude of the vector $\bar{V}_a = \bar{V}_I - \bar{V}_w$. The Earth is assumed to be flat and \bar{V}_I is the velocity of the aircraft with respect to an Earth-fixed inertial coordinate system; \bar{V}_w is the velocity of the mean wind with respect to the same system. Thus the definition of kinetic energy in equation (1) eliminates the effects of constant winds from the total energy. Resolving \bar{V}_I into components along and normal to \bar{V}_a and equating to the approximate forces gives the following quasi-steady state equations of motion

$$m\dot{V}_a = T \cos(\alpha + \nu) - D - (mg) \sin \gamma_a - m(\dot{V}_w)_{at} \cos \gamma_a \quad (3)$$

$$mV_a \dot{\gamma}_a = [T \sin(\alpha + \nu) + L] \cos \phi - mg \cos \gamma_a - m(\dot{V}_w)_{at} \sin \gamma_a \quad (4)$$

$$\dot{h} = V_a \sin \gamma_a \quad (5)$$

$$\dot{S} = V_a \cos \gamma_a + V_{wat} \quad (6)$$

where V_{wat} and $(\dot{V}_w)_{at}$ are the components of \bar{V}_w and $\dot{\bar{V}}_w$, respectively, along the horizontal projection of \bar{V}_a . Note that the vertical component of \bar{V}_w is assumed to be zero.

In the remainder of the discussion of the energy-rate model it is assumed that $\cos \gamma_a \approx 1$, $\sin \gamma_a \approx \gamma_a$, and that $\dot{\gamma}_a$ is negligible. (Later, when eq. (6) is integrated to find distance along the reference flightpath, $\cos \gamma_a$ is retained.) Using these assumptions and substituting for \dot{h} in equation (5) from (2) gives

$$\dot{E} = V_a \gamma_a + \frac{V_a}{g} \dot{V}_a \quad (7)$$

and combining (3) and (7) results in

$$\dot{E} = V_a \left[\frac{T \cos(\alpha + \nu) - D}{mg} - \frac{(\dot{V}_w)_{at}}{g} \right] \quad (8)$$

which is an alternative expression for energy rate. The wind-shear term in equation (4) is small compared with the gravity term and will be neglected; therefore, setting $\dot{\gamma}_a$ to zero results in the constraint

$$T \sin(\alpha + \nu) + L = W \quad (9)$$

where, by definition, $W = mg/\cos \phi$. This definition is used for convenience because it causes the effect of the bank angle on the energy-rate diagrams to appear as a change in aircraft weight.

Finally, equations (7) and (8) can be nondimensionalized by dividing them both by V_a . The resulting quantity on the left side, \dot{E}/V_a is defined as the normalized energy rate \dot{E}_n , and the two equations become

$$\dot{E}_n = \gamma_a + \frac{\dot{V}_a}{g} \quad (10)$$

and

$$\dot{E}_n = \frac{T \cos(\alpha + \nu) - D}{mg} - \frac{(\dot{V}_w)_{at}}{g} \quad (11)$$

Equation (11) specifies the energy rate as a function of the difference between thrust and drag, subject to the constraint that lift equals weight. Thrust and drag are in turn functions of the controls which produce forces in the direction of the airspeed vector \vec{V}_a . These controls are: the power setting π , the flap angle δ_f , the angle ν of the vectored thrust nozzle, and the angle of attack α . Equation (10) determines the relationship between flightpath angle and acceleration for the energy rate calculated from equation (11). Equation (10) indicates that a given energy rate may be utilized to fly at flightpath angle γ_a with constant airspeed, or to fly at zero flightpath angle with acceleration \dot{V}_a . An infinity of other combinations of γ_a and \dot{V}_a can also be chosen to yield the same energy rate. This makes possible a simplifying dichotomy in the trajectory synthesis; namely, that at any time the desired energy rate is selected by choice of appropriate controls, the linearly related quantities of γ_a and \dot{V}_a can be selected to generate the specifics of the flightpath. The next section develops the functional dependence of energy rate on the force-producing controls.

SELECTION OF REFERENCE CONTROLS

Since the STOL aircraft studied in this paper has four controls to achieve a specified energy rate and to maintain lift equal to weight, there is an excess of two controls over the minimum number needed for simultaneous solutions to equations (9) and (11). These two extra degrees of freedom in the controls are exploited to minimize power setting and, therefore, fuel flow at every energy rate. This optimization problem is restated in equivalent form as the maximization of energy rate for a given power setting:

$$\dot{E}_n(\pi) = \max_{\nu, \alpha, \delta_f} \frac{T \cos(\alpha + \nu) - D}{mg} \quad (12)$$

$$\text{Constraint: } T \sin(\alpha + \nu) + L = W \quad (13)$$

Because $(\dot{V}_w)_{at}$ and ϕ are not functions of the aircraft states or controls they are assumed to be zero for the maximization. The maximization must obey the following inequality constraints on the controls:

$$-10.5^\circ \leq \alpha \leq 19.5^\circ$$

$$6^\circ \leq \nu \leq 100^\circ$$

$$5.6^\circ \leq \delta_f \leq \delta_{f_{max}}$$

where $\delta_{f_{max}}$ is defined as the minimum of the placard value, or 65° . In addition, a lift or "maneuver" margin is required to guarantee sufficient reserve normal force for changing the flightpath (in emergencies) by an increase in angle of attack alone. This constraint takes the form

$$\frac{L(\alpha_{max}) + T \sin(\alpha + \nu)}{W} - 1 \geq \Delta n(\delta_f) \quad (14)$$

Pilots familiar with the test aircraft (AWJSRA) specify that Δn be at least 0.4 for $\delta_f \geq 30^\circ$ and 0.69 for $\delta_f = 5.6^\circ$, the minimum flap deflection. As a result of pilot comments after early flight tests, the minimum value of Δn was increased to 0.5.

The use of equation (12) converts the problem from one of finding the minimum power setting for a given energy rate to one of finding the maximum energy rate for a given power setting. The solution is found by holding π fixed and adjusting δ_f and ν to maximize \dot{E}_n , the angle of attack being adjusted to satisfy the constraint specified by equation (13). The minimum energy rate attainable from equation (12) is the maximum energy rate attainable with minimum power setting; namely, the greater of flight-idle or the minimum power required to satisfy the maneuver-margin. However, energy rates more negative than those attainable from equation (12) are also of interest.

At a particular airspeed with the power setting fixed at its minimum, more negative values of E_n may be obtained by increasing v, δ_f , or both beyond the values obtained from equation (12). Since the values of δ_f and v for a given value of E_n are not unique and fuel consumption cannot be reduced further, a different criterion is needed for selecting δ_f and v . The criterion chosen is minimization of noise. Because noise under the aircraft is known to increase as the nozzles producing the vectored thrust are turned downward, a decrease in energy rate beyond the minimum value from equation (12) is achieved by increasing the flap angle to its limit, or placard value, before the nozzle angle is increased.

The result of applying these procedures to the AWJSRA is shown in figure 1 for a weight of 38,000 lb, sea-level altitude, and standard temperature. The figure gives the envelope of energy rate vs equivalent airspeed V_{EQ} , with throttle, flaps, and vectoring nozzles as parameters. Each of the small circles indicates values of V_{EQ} and E_n that are stored in the onboard computer along with the corresponding values of v, δ_f , and α . To avoid cluttering the figure, angle of attack is not plotted; it will be discussed separately. At any airspeed, the $E_{n_{max}}$ and $E_{n_{min}}$ curves define the range of permissible energy rates. The optimum controls for a given airspeed and energy rate are determined by interpolation between contours of constant controls. For example, at an airspeed of 105 knots and $E_n = -0.17$, the optimum controls are found to be $\delta_f = 26^\circ, v = 6^\circ$, and $\pi = 84\%$ (point A, fig. 1); angle of attack (not shown) is 9.4° . Maximum energy rate with minimum thrust occurs at 112 knots (point B) and corresponds approximately to $(L/D) = 10$.

It should be noted that the force-producing controls in this experimental STOL aircraft have unusual characteristics that account for the relative complexity of figure 1. Throttle affects both lift and drag at all speeds, but the effect on lift is greatest in the STOL regime below about 80 knots. The thrust magnitude produced by the vectoring nozzle, referred to as the hot thrust, is also controlled by the throttle and accounts for about 60% of the total thrust produced by the two engines. The remaining 40% of the thrust, which is the cold thrust produced by the fans, energizes the augmentor wing to increase lift at STOL speeds.

The relationship between the controls and the energy rate is revealed more clearly in figure 2 at the example airspeed of 105 knots. Many such plots at various airspeeds would be required to illustrate the complete dependence of the controls on energy rate. As the energy rate decreases below its maximum value of 0.28, throttle decreases nearly linearly until idle throttle is reached. In this interval, flaps increase only slightly while nozzle angle remains at minimum and angle of attack increases. At more negative energy rates, flaps become the dominant control until they reach the placard value of 40° at this airspeed. Angle of attack decreases sharply as flap angle increases. Finally, nozzle angle increases toward its maximum value of 100° as the energy rate decreases toward its negative limit of -0.3.

The envelope of values of angle of attack corresponding to the data in figure 1 is plotted vs equivalent airspeed in figure 3. The maximum nozzle contour is also the contour of minimum α . At low speeds the maximum

angle-of-attack contour coincides with the maximum-power contour until the latter intersects the 30°-flap contour. As speed increases beyond that point, the maximum α lies on the 30°-flap contour and the corresponding power decreases to its minimum of 84%. At still higher speeds, the maximum angle-of-attack contour coincides with the flight-idle power contour.

The significance of the 30°-flap setting may be seen more clearly by referring back to figure 1, where the contour of maximum α can be traced as follows: Start on the 84% power contour at maximum speed and follow that contour, past point B, to its intersection with the 30°-flap contour. From there proceed along the 30°-flap contour to the maximum-power contour and along the latter to the minimum speed (where the maximum-power contour becomes vertical). It was found while generating the data for the energy-rate tables that the maximum value of α becomes increasingly sensitive to the minimum value of maneuver margin as airspeed decreases.

In the flight implementation of the algorithm, data tables corresponding to four diagrams such as that shown in figure 1 are utilized, two for sea-level altitude at weights of 38,000 and 48,000 lb and two others for the same weights at an altitude of 5,000 ft. Figure 4(a) shows the diagram for an aircraft weight of 48,000 lb at sea level; figure 4(b) shows the effect of altitude on energy rate by superimposing energy-rate diagrams for zero and 5,000-ft altitudes at a weight of 38,000 lb. The effect of weight is seen to be much greater than that of altitude over the altitude range of interest. However, the 5,000-ft altitude was selected on the basis of the flight-test environment and could probably be increased to 10,000 ft without significant loss in accuracy. Experience indicates that these are sufficient data for adequate interpolation of the contour. Each table requires 124 words of memory in the airborne computer.

These tables are generated for a specified ambient temperature; no mean winds are assumed. The data are corrected during trajectory synthesis for the best available estimates of the temperature and wind profiles, using methods described in the next section.

TRAJECTORY SYNTHESIS

In the preceding section the criteria of fuel conservation and noise reduction were used to determine the four reference controls of throttle, nozzle angle, flap angle, and angle of attack as functions of the energy rate. This approach replaced the problem of selecting four control variables with the simpler problem of selecting a single, equivalent variable, namely, the energy rate. In this section the energy-rate variable is used in generating efficient terminal-area trajectories.

The problem of terminal-area-trajectory synthesis can be stated as the specification of rules for flying an aircraft with initial state vector $(X_i, Y_i, h_i, H_i, V_i)$ to a final state vector $(X_f, Y_f, H_f, h_f, V_f)$. To be of practical interest, such rules must generate efficient and flyable trajectories

connecting various initial and final state vectors. By specifying a performance criterion, such as fuel consumption, this problem can be fit into the framework of optimal control theory. However, the difficulty of solving an optimal control problem characterized by a five-element state vector makes this approach computationally impractical for in-flight implementation. Following reference 6, the synthesis problem has been separated into two essentially independent problems. The first problem consists of synthesizing a horizontal or two-dimensional (2D) trajectory that matches the initial position and heading (X_i, Y_i, H_i) to the final position and heading (X_f, Y_f, H_f) . The second problem, solved after the horizontal trajectory has been computed, consists of synthesizing efficient speed and altitude profiles that match the initial and final speeds and altitudes, (V_i, h_i) and (V_f, h_f) , respectively.

Synthesis of Horizontal Flightpaths

References 6 and 7 give several algorithms for computing near-minimum distance two-dimensional trajectories as a sequence of an initial constant-radius turn, a segment of straight flight and a final turn, where the radii are chosen so as to avoid exceeding a specified maximum bank angle at the maximum ground speed encountered in the turn. A new algorithm was developed for flight implementation in the present study. This algorithm, which is derived in reference 2, is based on the solution of a set of closed-form equations; it will always yield a solution. Figure 5 illustrates the two-dimensional trajectories computed by the algorithm for several initial positions P_i in the terminal area. Note that the terminal point P_f lies on an extension of the runway centerline, and that the heading angle H_f of all trajectories is equal to the runway heading at that point. Thus, the algorithm always generates two-dimensional trajectories that match the initial and final state vector components - (X_i, Y_i, H_i) and (X_f, Y_f, H_f) . Note that the point P_f in figure 5 need not necessarily be at the beginning of the final approach. As in reference 6, a fixed horizontal approach path may be specified by a series of input waypoints, and P_f may be located at any of those waypoints. That portion of the synthesized horizontal trajectory between P_i and P_f is referred to as the "capture" trajectory.

Synthesis of Speed-Altitude Profiles

The horizontal distance of the trajectory S , a known quantity computed in the previous step, adds a third boundary condition to be satisfied by the profiles. Although this three-state (S, h, V_a) optimal-control problem is much simpler to solve than the original five-state problem, it is still too complex for onboard-computer implementation. A simpler algorithm was therefore developed that generates near-optimum speed-altitude profiles by matching the general characteristics of optimum fuel and noise trajectories studied in references 5 and 8, respectively. We briefly explain the rationale for this algorithm with reference to descent, which is the most difficult case.

It was found in reference 5 that the descent portion of a minimum-fuel-descent trajectory is characterized by a delay in the start of the energy decrease for as long as is possible, consistent with meeting end constraints

on speed and altitude. Furthermore, the energy change consists initially of descent to the final altitude at near-constant indicated airspeed, followed by a rapid airspeed deceleration in level flight. Most of the energy change takes place at minimum throttle, as one might expect for minimum-fuel flight. Minimum-noise-descent profiles computed in reference 8 are similar in that they also delay the start of energy decrease as long as possible, but they approach the final altitude in a steep descent to maximize the aircraft's altitude above the ground near the runway. This means that the deceleration to the final airspeed takes place before the start of descent or during the early portion of the descent. Thus the two types of descent profiles differ primarily in the way they proportion the use of available energy rate to decrease altitude and airspeed.

To facilitate the synthesis of such profiles, a family of decreasing (and by extension, increasing) energy profiles, which includes the two types described as special cases, is defined by two parameters σ and ϵ . The first parameter, σ , selects the fraction of minimum or maximum available energy rate ($\dot{E}_{n_{\min}}$, $\dot{E}_{n_{\max}}$) to be used for decreasing or increasing energy, respectively. The values of $\dot{E}_{n_{\min}}$ and $\dot{E}_{n_{\max}}$ can be read from figure 1 at each equivalent airspeed. The second parameter, ϵ , determines the fraction of the selected energy rate to be used for deceleration or acceleration. Then, for particular choices of σ and ϵ , the energy rate, airspeed, flightpath angle, altitude, and horizontal distance are computed for decreasing energy as follows:

$$\dot{E}_n = \sigma \dot{E}_{n_{\min}} \quad 0 \leq \sigma \leq 1 \quad (15)$$

$$\dot{V}_a = g\epsilon \dot{E}_{n_{\min}} \quad 0 \leq \epsilon \leq 1 \quad (16)$$

$$\gamma_a = (1 - \epsilon) \dot{E}_n \quad (17)$$

$$\dot{h} = V_a \gamma_a \quad (18)$$

$$\dot{S} = V_a \cos \gamma_a + V_{wat} \quad (19)$$

Profiles for increasing energy can be computed by replacing $\dot{E}_{n_{\min}}$ with $\dot{E}_{n_{\max}}$. Decreasing or increasing energy profiles are generated by integrating equations (16), (18), and (19) for particular choices of σ and ϵ .

It will be recalled that the wind-shear term in equation (11) was assumed to be zero in the generation of the energy-rate tables. The effects of that term are accounted for by rewriting equation (15) as

$$\dot{E}_n = \sigma \dot{E}_{n_{\min}} - \frac{(\dot{V}_w)_{at}}{g} \quad (20)$$

It is assumed that the magnitude and direction of the wind are functions of only the altitude and that the vertical component of the wind is zero. Then from the chain rule

$$(\dot{V}_w)_{at} = \frac{\partial V_{wat}}{\partial h} \dot{h} \quad (21)$$

and substituting for \dot{h} from equations (17) and (18)

$$(\dot{V}_w)_{at} = \frac{\partial V_{wat}}{\partial h} \left[\frac{V_a}{g} (1 - \epsilon) \dot{E}_n \right] \quad (22)$$

Substituting for $(\dot{V}_w)_{at}$ in equation (20) and solving for \dot{E}_n gives

$$\dot{E}_n = \frac{\sigma \dot{E}_n \min}{1 + \frac{\partial V_{wat}}{\partial h} \frac{V_a}{g} (1 - \epsilon)} \quad (23)$$

or

$$\dot{E}_n = \frac{\sigma \dot{E}_n \min}{1 + A_{kw} (1 - \epsilon)} \quad (24)$$

where

$$A_{kw} = \frac{V_a}{g} \frac{\partial V_{wat}}{\partial h}$$

is computed by a wind estimation algorithm. Equation (24) replaces (15) in the profile synthesis outlined above.

An additional constraint was imposed on the synthesis because the auto-flap servo does not allow reversal of the flap motion. Thus, reference trajectories calling for extension and subsequent retraction must be avoided. The problem is solved at higher speeds by setting the lower limit on \dot{E}_n to its value on the 84%-throttle contour if the airspeed at the next waypoint (nearest touchdown) is greater than that at point B in figure 1. At lower speeds any reversal in reference flaps is kept small by maintaining a continuous descent (negative γ) during flap extension.

To illustrate the effect of the parameter ϵ on the descent-deceleration profiles assume $\dot{E}_n = -0.13$, independent of speed, and let the airspeed that is to be achieved at touchdown be 100 ft/sec. To achieve the desired boundary conditions, equations (16), (18), and (19) are integrated in backward time starting with the speed and altitude at touchdown. The resulting airspeed and altitude profiles are plotted as a function of distance to touchdown in figure 6 for $\epsilon = 1, 0.5, \text{ and } 0.0$. The profile for $\epsilon = 1$ is seen to approximate the minimum-fuel descent, that for $\epsilon = 0$ approximates the minimum-noise descent, and the profile for $\epsilon = 0.5$ is a compromise between fuel and noise minimization.

The algorithm used in reference 5 to find minimum-fuel trajectories would require too much computation time for implementation as part of the AWJSRA flight system. Therefore, the approach used here is to make the required energy changes at the maximum allowable rate (i.e., at the maximum $|\dot{E}_n|$). Simulation studies indicate that a further fuel reduction (of from 5% to 10%) could be achieved by proper scheduling of σ and ϵ , but this is a subject for future study. The use of the maximum $|\dot{E}_n|$ yields minimum time and minimum noise, and is the most stringent test of the capabilities of the guidance system, since it is generally operating along constraint boundaries.

These trajectories are obtained by setting σ to unity and thereby following the $\dot{E}_{n_{\min}}$ contour during descent and deceleration. However, for the aircraft under study this choice of σ yields energy rates too negative for safe operation in the terminal area at some airspeeds. A limit less than 1.0 is also necessary to reserve energy rate for perturbation control. A practical upper limit on σ is about 0.9 for the AWJSRA. In the flight implementation, the two profile parameters are keyboard entries that allow the pilot to choose values appropriate for each landing approach. In addition, the pilot can specify the maximum deceleration and descent angles via keyboard entry. The maximum safe deceleration for this aircraft is limited to about 0.06 g by the maximum rate at which flaps can be extended. The synthesis algorithm is configured to decrease σ below its limit if that is necessary to satisfy these constraints.

For simplicity the speed-altitude profile has been treated as a straight approach along the runway centerline. In the more general situation the distance from touchdown is the distance along a horizontal path composed of both turns and straight segments, for example, those in figure 5. The effect of the turns on the speed-altitude profile is small and is accounted for by approximately modifying the aircraft weight, as in equation (9).

The technique described above generates an increasing (in backward time) energy-profile starting at the desired final speed and altitude. A complete synthesis of the descent trajectory requires rules for matching this profile to the initial speed and altitude of the aircraft. The freedom of the aircraft to maneuver in altitude is restricted by air traffic control as well as by passenger comfort considerations. Thus, as an aircraft approaches a terminal area, it is generally not allowed to climb above its initial approach altitude for the purpose of optimizing the approach trajectory. The aircraft must hold this altitude until starting the final descent. However, while flying at altitude h_i , it may change to a new airspeed V_{TA} , called the terminal-area speed; V_{TA} can be higher or lower than the initial speed V_i . Unless specified by the pilot via keyboard entry, it is chosen to minimize fuel use per unit distance, and is 140 knots for this aircraft (it would be 220 to 250 knots for conventional jet transports).

The various rules contained in the preceding two paragraphs can now be combined to yield the complete algorithm. The vertical synthesis begins with the forward integration from the initial aircraft velocity and altitude. If V_i and V_{TA} are not equal, ϵ is set to unity until V_{TA} is achieved, after which σ and ϵ are set to zero and the integration proceeds at constant speed

to the end of the initial turn. The turn may, of course, be completed before the speed change, in which case the integration continues until V_{TA} is achieved. The forward integration is followed by the backward-time integration from final conditions (h_f, V_f) using the specified σ and ϵ . If the altitude reaches its target value of h_i before the airspeed reaches its target value, V_{TA} , ϵ is set to unity, forcing the flightpath angle to zero, and the energy rate is used entirely for accelerating (in backward time) toward V_{TA} . On the other hand, if the airspeed reaches its target value first, then ϵ is set to zero and the energy rate is used entirely for increasing altitude until h_i is reached. When the target values of both airspeed and altitude have been achieved, σ is set to zero, that is, $\dot{E}_n = 0$. Let S_h be the total length of the horizontal path and let S_f and S_b be the distances of forward and backward integrations, respectively. A valid trajectory has been generated if the cruise distance S_c , computed from

$$S_c = S_h - S_b - S_f \quad (25)$$

is nonnegative, that is, if $S_c \geq 0$. If S_c is negative, the synthesis has failed because the aircraft is too close to the capture point P_f .

Figure 7 illustrates the various segments of an approach trajectory synthesized by the algorithm. As before, it is assumed for simplicity that $\dot{E}_n = -0.13$, a constant. Other parameters defining the problem are indicated in the figure. Note that the descent angle decreases from an initial value of -7.5° to -3.75° to allow the aircraft to decelerate. The reference controls for this trajectory can be interpolated from figure 1. The dashed vertical lines in figure 5 indicate points where the flightpath angle, airspeed rate, or heading rate change instantaneously, thereby calling for instantaneous changes in the reference controls. At each of these points, referred to as "command points," the information necessary to initialize the real-time forward integration in the track mode, which will be discussed in the next section, is stored in the "command table."

The profile depicted in figure 7 is for an approach trajectory consisting of a capture trajectory followed by a single segment of fixed flightpath from P_f to touchdown. As was mentioned earlier, this fixed path can be expanded by adding a number of fixed waypoints, each having a specified speed and altitude. The speed and altitude profiles between adjacent waypoints are synthesized in fast-time using the same algorithm as for the capture trajectory. The synthesis is done entirely in backward time, starting at the final waypoint and ending at the capture waypoint. The altitude and speed at waypoint N determine the initial condition and those at waypoint $N - 1$ determine the final conditions, that is, those to be captured, in the backward-time synthesis.

If during synthesis of the speed-altitude profile along the fixed trajectory either the speed or altitude fails to reach (capture) the target value specified at a waypoint, the values attained are accepted and the new target values become those specified at the next waypoint. This choice of the synthesis logic contributes to a smooth and versatile operation. For example, it allows the pilot to change the minimum flightpath angle between waypoints without a cumbersome change in the X, Y coordinates of the waypoints. It

also minimizes the occurrence of failure-to-capture conditions, which pilots consider a nuisance. Of course, the pilot must be informed of actual speeds and altitudes achieved at the waypoints by the synthesis.

Lead Distances

Since the controls cannot change instantaneously, it is desirable to provide some warning of such impending changes in the track mode, discussed in the next section. Using the method of reference 7 and assuming that a control will change at its maximum rate, $|\dot{C}|_{\max}$, a lead distance is computed as

$$\Delta S = \frac{k_{LC} \Delta C V_{GR}}{|\dot{C}|_{\max}}$$

where ΔC is the desired instantaneous change in the control and V_{GR} is the reference groundspeed. The lead distances are stored in the command tables for use at the appropriate command points.

Temperature Compensation

It is well known that the performance of jet engines in terms of thrust vs rpm is strongly dependent on ambient temperature and barometric pressure. Mach number, while significant at high speed, is of secondary importance within the flight envelope of the AWJSRA. It was noted earlier that the energy-rate diagrams are generated for two altitudes at different weights, thus under the implicit assumption of a known relationship between altitude, temperature, and pressure. The most commonly used relationship, the standard atmosphere, treats the absolute ambient temperature as a linear function of the pressure altitude for altitudes as high as 36,000 ft. The actual ambient temperatures encountered at the flight-test site can usually be approximated by such a linear relationship although it may differ markedly from the standard value at a given pressure altitude. Since it is impossible to know in advance what the actual temperature profile will be, the system must be capable of accounting for temperature deviations from the value T_S used in generating the energy-rate diagrams. This could be done by making temperature an additional parameter of the energy-rate tables; however, the amount of stored data would be doubled and the computation time would be substantially increased. An alternative approach, used here, is to use the energy-rate data as though there were no temperature deviation and then to adjust the reference power setting to compensate for the temperature difference.

This approach is possible because both hot and cold thrust can be approximated in the following piecewise linear form:

$$\tau = \tau_1 + \frac{K_1(\pi - \pi_1)}{\sqrt{\theta_2}} \quad (26)$$

where the subscript i refers to the next lower value of π for which energy-rate data are stored. Assuming negligible Mach number effects, $\theta_2 = T_a / T_0$, where T_a is the actual ambient temperature and T_0 is the standard temperature at sea level. It can be seen from equation (26) that if each value of π is replaced by $\pi^* = \pi \sqrt{T_a / T_S}$, the thrust and hence the remaining controls and E_n will be approximately the same as obtained from the energy-rate data when $T_a = T_S$. One precaution required in the synthesis is to limit the value of E_n such that π^* will not exceed the allowable maximum. In addition, T_S should be chosen so that it will never exceed the value of T_a . This will prevent π^* from being less than the flight-idle value of 84%, which is a hardware constraint independent of temperature.

Temperature Profile Estimation

The ambient temperature profile is estimated assuming a constant lapse rate between the runway and the cruise altitude. The runway temperature is entered by keyboard. The "cruise altitude" is the current pressure altitude when the synthesis mode is engaged and the estimated ambient temperature is calculated from the total air temperature measured by the STOLAND system. This model was satisfactory for conditions encountered in the flight tests, but several linear segments might be needed for a greater range of altitudes.

Wind Profile Estimation

The wind magnitude and heading at prescribed altitudes are stored in the computer. For flight tests the data were obtained by radar tracking of a weather balloon launched a few minutes prior to flight. Prior to the start of synthesis calculations the Cartesian components of the wind and their partial derivatives with respect to altitude are computed and stored. These data are subsequently used to compute the along-track component of the wind, the wind-shear term in E_n and the reference inertial and groundspeeds.

Computation Time

The integration step size used in the synthesis is 1 sec during deceleration or acceleration, 2 sec for descent and turns at constant speed, and a single step for segments of straight and level constant-speed flight. The entire synthesis on the STOLAND airborne computer requires about 2% of the time required for the aircraft to fly the same trajectory. The elapsed (clock) time is about double this value because computation is carried out in far background, that is, in time left over from the autopilot and other requirements of the basic STOLAND system. Thus, synthesis of a trajectory that will be flown in 6 min requires from 6 to 8 sec.

REAL-TIME TRAJECTORY GENERATION: TRACK MODE

After a profile has been synthesized and the pilot has elected to fly it by engaging the track mode, the reference states and controls for that profile are generated in real time. If an onboard computer had sufficient memory capacity to store all of the reference states and controls during fast-time synthesis at small intervals of time, this logic would not be required. However, limitations on the storage available in the STOLAND computer made this approach impractical. To minimize memory usage, a different method was implemented at the expense of increased complexity of computation. The method consists of storing reference trajectory data generated in the predictive mode at the "command points," as defined earlier. Between "command points" the reference trajectory is generated in real time by the same integration logic used during fast-time synthesis; however, the integration is now done entirely in forward time. Generation of a flyable reference trajectory that meets the desired boundary conditions is guaranteed because it is a precise repetition of a previously successful synthesis.

The real-time forward integration uses distance along the ground track as the independent variable. This is accomplished by finding the vector distance \bar{s} covered by the aircraft in a given small time interval. The projection of \bar{s} along the reference horizontal path is used as the integration step size for the reference trajectory computation. The integrated or dependent variables are reference time, airspeed, altitude, and heading. The time error between the reference and actual, or "clock," time replaces the along-track error encountered with a time-based reference trajectory. The choice of distance rather than time as the independent variable gives a more flexible and operationally improved system. The reasons for this are as follows. In a distance-based reference trajectory system, the aircraft will track the reference airspeed and altitude regardless of winds as it flies along the ground track. It is not necessary to null time errors if time control is not required. The system can thus be operated either in a three- or a four-dimensional tracking mode, depending on whether the time-error loop is open or closed. This flexibility is lacking in a time-based reference trajectory system, where only the four-dimensional tracking mode is possible. In the time-based system, if the actual winds differ significantly from the forecast winds used in fast-time trajectory synthesis, the aircraft controls may have insufficient authority to track the reference position; this results in unacceptable tracking characteristics.

One difficulty with the distance-based reference trajectory is that distance along the trajectory does not necessarily increase monotonically with time. Large navigation errors can cause the new reference position to fall behind the previous one or to move ahead with a large step. This can result in control-system saturation during the critical descent and deceleration segments. The system therefore contains logic to limit the change in reference position during each integration step to the equivalent of 60% to 140% of the current reference groundspeed.

In order to reduce computation time, a major portion of the real-time reference trajectory computation is done in far-background, using integration steps comparable to those used in the synthesis. The resulting variables, such as the reference controls, are computed and stored for a short interval ahead of the reference position. Only quantities required for the perturbation control law are computed in foreground, using small integration steps. The details of this procedure are discussed in the section on computer implementation.

PERTURBATION CONTROL LAW

Perturbations of the aircraft states from the reference states are used in the control law to generate perturbation controls which are added to the reference controls in order to null errors in airspeed, altitude, and cross-track position. The feedback states in the control law also include cross-track error rate and flightpath angle as well as the integrals of airspeed and altitude errors. The latter two are used to reduce speed and altitude bias errors caused by inaccuracies in the stored energy-rate data and errors in the estimates of wind and temperature profiles.

The controls are nozzle, pitch, roll angle, and power setting. Flaps are not used as perturbation controls because of their relatively low rate limit and an operational constraint that flap motion be monotonic during an approach. The flap command is simply the reference value at each ground track position, limited to the placard value at the current airspeed.

Lateral perturbation control is essentially uncoupled from the longitudinal mode and is accomplished through a roll-angle command to the roll-command autopilot. This command is of the form

$$\phi_c = \phi_r + k_{\phi y} y + k_{\phi \dot{y}} \dot{y} \quad (27)$$

where ϕ_r is the reference roll angle, and y and \dot{y} are the crosstrack error and error rate, respectively. The two gains were chosen to provide a well-damped response and control activity compatible with the noise characteristics of the navigation system.

Longitudinal perturbation control for correcting airspeed and altitude errors is difficult because the reference controls generated by the energy-rate schedule of figure 1 often lie on a constraint boundary and therefore cannot be perturbed freely in both directions. The two controls that are often constraint-limited during a fuel-conservative approach are power setting, π , and nozzle angle, v . Some insight into this problem can be obtained using data from the energy-rate schedules. Figure 6 shows the energy-rate envelope from figure 1, with the minimum reference nozzle and minimum reference throttle constraint boundaries. These boundaries divide the envelope into four regions: region I, in which v cannot be reduced; region II, in which neither π nor v can be reduced; region III, in which π cannot be reduced; and region IV, in which π and v are free to move in either direction. The combinations of

controls available for increasing and decreasing \dot{E}_n in each region are indicated in the figure. Note that in region I, nozzle could be used as an additional control variable for decreasing energy rate. However, this variable is not used because throttle and pitch provide adequate control of flightpath errors in this region. In region IV the minimum reference throttle is above idle and is determined by the maneuver margin constraint. At each airspeed in this region the negative throttle perturbation that can be added to the reference power setting to yield the commanded setting is limited to -2% for safety reasons. Positive and negative power perturbations are further limited so that the commanded power setting π_c falls within the engine operating range, $84\% \leq \pi \leq 96\%$.

The longitudinal perturbation equations and the perturbation control law can be written in state vector notation as

$$\frac{dx}{dt} = Fx + Gu \quad (28)$$

$$u = Kx \quad (29)$$

where

$$x = (\Delta V, \Delta \gamma, \Delta h, \int \Delta V dt, \int \Delta h dt)^T$$

$$u = (\Delta \pi, \Delta \theta, \Delta v)^T$$

The delta quantities are the perturbations from reference values, that is, $\Delta V = V - V_{ar}$, etc., where V_a and V_{ar} are the aircraft and reference true airspeeds, respectively. The commanded controls are the sum of reference and perturbation controls:

$$u_c = (\pi_r + \Delta \pi, \theta_r + \Delta \theta, v_r + \Delta v)^T \quad (30)$$

For a powered-lift STOL aircraft, such as the one used for these flight tests, the values of F and G are strongly dependent on airspeed and energy rate and are thus time-varying along a trajectory. Quadratic optimal synthesis would therefore yield time-varying gain matrices that are also functions of the reference trajectory. But it is neither practical nor necessary to implement a complex, reference-trajectory-dependent gain matrix in order to achieve adequate control system performance in this case.

The design procedure employed here began by first computing optimum gain matrices at various operating points in the control region diagram (fig. 6), using fixed values of F and G . The analysis of these gain matrices showed the strongest dependence on airspeed, reference nozzle angle, and reference flap. Sensitivity of the closed-loop eigenvalues to changes in several of the gains was low, allowing those to be set to zero or held constant throughout the operating region. It was possible to fit the variable gains with relatively simple functions of reference airspeed, nozzle angle, and flap angle. This method resulted in the following gain matrix:

$$K = \begin{bmatrix} \frac{-40}{V_{ar}} & \frac{-40}{V_{ar}} & \frac{-8}{V_{ar}} & \frac{-4 \cos v_r}{V_{ar}} & \frac{-0.6}{V_{ar}} \\ 0 & -0.4 & \frac{-14}{V_{ar}} & 0 & \frac{-0.2}{V_{ar}} \\ 3 & 2 & 0.6 & 0.3 & 0.5 \max \left\{ 0, \frac{\delta_f - 45^\circ}{20} \right\} \end{bmatrix} \quad (31)$$

where V_{ar} is in units of ft/sec. Extensive computer calculations have verified that the closed-loop eigenvalues of this system have damping factors of 0.707 or greater and real parts less than $-0.05/\text{sec}$ at all operating points.

These characteristics provide adequate tracking performance. When operating in region I of figure 8 the last row of K is set to zero, since nozzle angle is not used for control. In regions II and III power setting perturbations are limited to positive values, and in region II nozzle perturbations are limited to positive values. In region IV each control moves freely, but negative power perturbations are limited to -2% rpm, as previously explained. Control limiting can reduce the effectiveness of integral feedback of speed and altitude. Some design considerations for these integral feedback loops are given in reference 9.

The throttle and nozzle-angle perturbations generated by the control law will generally be of opposite sign, because the signs of the elements in the first row of K are opposite of the signs of the third-row elements. Thus, even in region II, where throttle and nozzle perturbations are each limited to move only in the positive direction, they are not generally limited simultaneously. This implies that two controls, either throttle and pitch or nozzle and pitch, are free to move. Transient response studies using a non-linear simulation of the aircraft and guidance system have shown that the control power is adequate to provide rapid and well-damped airspeed and altitude error responses in region II.

STRUCTURE AND OPERATION OF THE FLIGHT SYSTEM

The implementation of the flight system is based on two modes of operation. In the first mode, referred to as the "predictive" mode, new trajectories are synthesized one after the other as rapidly as possible so long as the system is in the predictive mode. Upon completion of each synthesis the system checks to determine whether the pilot has called for the second, or "track," mode to be engaged. If such is the case the predictive mode is terminated. The most recently synthesized trajectory is regenerated in real time and tracked in real time by the closed-loop guidance law.

The organization of the functional units of the system is shown in figure 9. When the pilot activates the system through the mode-select panel, the fixed horizontal flightpath is displayed as a solid line on the multifunctional

display (MFD). This display operates in conjunction with the navigation system to give a map-like view of the terminal area (see ref. 1 for details on this device). A triangular symbol indicating the aircraft position and heading appears on the display when a valid navigation mode has been selected. Next, the pilot selects the capture waypoint by keyboard entry. Then computations begin in the fast-time trajectory synthesis module. If a trajectory is successfully synthesized, it is stored at command points, as previously explained, and the horizontal capture path is displayed as a dashed line.

Although the capture-trajectory algorithm synthesizes successful trajectories for a wide range of initial conditions, there are conditions where it will fail to do so. For example, if P_i in figure 5 is very close to the capture waypoint P_f , then the algorithm can fail because there is insufficient distance along the computed minimum distance path to complete the required change in speed or altitude or both. In that case, the reason for the failure to synthesize is displayed as a short message on the MFD. The pilot can correct the failure-to-capture condition by flying the aircraft away from the capture waypoint or by selecting a more distant capture waypoint.

Figure 10 gives an example of trajectories displayed on the MFD. The solidly drawn track is the fixed or prestored reference trajectory on which waypoint numbers are indicated. The pilot has selected waypoint 3 as the capture waypoint. The track drawn as a dashed line from P_i to waypoint 3 indicates to the pilot that a valid capture trajectory has been computed and that the track switch is armed. If the synthesis is not successful or if the track mode is not engaged the routine is reentered, as shown in figure 9, with updated aircraft states as the new initial conditions. The speed-altitude profile is computed for both the fixed and capture portions of the trajectory until a successful synthesis has been achieved. Then the reference states at the capture waypoint are stored and (only) the capture trajectory is resynthesized continuously as the aircraft moves. If the capture waypoint is changed, the speed-altitude profile synthesis is reinitialized including the fixed portion of the trajectory. Aircraft weight, runway temperature, the estimated wind profile, and the coordinates and speeds of the fixed waypoints may also be changed by keyboard entry, but the synthesis mode must be disengaged to make those changes.

To account for the distance the aircraft will travel while the trajectory is being synthesized, the capture trajectory is actually computed from a point, P_2 in figure 10, projected 15 sec ahead of the aircraft under the assumption that the aircraft will maintain straight constant-speed flight during that interval. If the aircraft actually maintains those conditions the initial errors will be small when tracking of the reference trajectory begins, and ample lead will be provided on the reference bank angle for initial turns. (Flight experience has indicated that it would be useful to allow for capture from turns. In that case the predicted flightpath from P_1 to P_2 would follow the circular arc defined by the initial aircraft states.)

Tracking of a synthesized trajectory is initiated when the pilot engages a switch, causing the system to enter the track mode. In this mode the reference states and controls for the synthesized trajectory are generated by the

technique of real-time integration, which was described in a previous section. At the same time the capture trajectory is frozen and changed to a solid line on the multifunction display (fig. 10). The perturbation control law is activated, thus initiating closed-loop tracking of the trajectory.

CONCLUDING REMARKS

The guidance system described in this paper uses the technique of fast-time onboard trajectory synthesis to provide fully automatic flight capability and near-optimal fuel conservation. This technique overcomes the performance limitations inherent in a stored, precalculated trajectory by adapting the trajectory to the unique conditions encountered in each landing approach. The ability to adapt is crucial in terminal-area operations because the initial conditions for the approach and the wind and temperature profiles are not predictable with sufficient accuracy prior to takeoff. The implementation of the algorithm on an airborne computer and subsequent flight tests have shown that the design technique described here is practical. Furthermore, the software structure developed here for a complex STOL aircraft can be adapted, with several simplifications, to conventional aircraft. Finally, the automatic control law could be replaced with a flight-director system to allow the synthesized trajectories to be flown manually.

APPENDIX

AIRBORNE COMPUTER IMPLEMENTATION

Background Computations

Most of the computation required for the fuel-conservative guidance system is carried out in far-background, that is, during the portion of each 50-msec computation cycle not required for the remainder of the onboard system. The tasks performed in far-background are the horizontal flightpath synthesis, speed-altitude profile synthesis, and a major portion of the real-time reference trajectory generation. The following sections discuss these tasks in terms of the subroutines that perform them. In addition, it is convenient to include that portion of the real-time reference trajectory generation done in foreground because of its close relationship to the background computations.

The background executive, DTG4D, controls the computations in far-background, as shown by the flow chart in figure 11; the various flags shown in the chart are defined in table 1. When DTG4D is first entered, the capture waypoint is set to zero and flags are set to indicate that the estimated wind and temperature profiles must be recomputed. Note that these and other flags used in background may be changed in foreground as the result of keyboard entries. Appropriate interlocks prevent keyboard entries that would disrupt calculations in progress. Subroutine WPBGND calls subroutine TWOD to synthesize the fixed 2D path and loads the data required for the cockpit display. Initially WAYCAL is nonzero and it is set to zero at the end of WPDGND. If a waypoint is changed by keyboard entry WAYCAL is set nonzero. Logic in the keyboard entry routines prevents the waypoints from being changed if REFP \neq 0, that is, if synthesis of the two-dimensional capture trajectory and the speed-altitude profiles are called for.

If IFIX is zero, the speed-altitude profile is synthesized for both the fixed and capture portions of the horizontal trajectory. When a successful synthesis has been completed the states at the capture waypoint are stored and IFIX is set to 1. Then the speed-altitude profile is synthesized only over the capture trajectory. If the profile synthesis fails, NOCAP is set to indicate the variable (speed or altitude) that is not attaining its target value and the synthesis is repeated.

If NOCAP = 0 the real-time reference trajectory generation is initialized and HORNAV is checked to see whether the pilot has engaged the track mode. In the track mode, NOMTRJ is called repetitively in the final loop in the flow-chart, unless the track mode is disengaged or an error condition is encountered (an unlikely event).

Horizontal Flightpath Synthesis

The fixed and capture portions of the horizontal path are synthesized in separate operations as noted in the discussion of DT4GD. However, the bulk of the computation for either portion is done by subroutine NEWPSI. The basic function of NEWPSI is to solve the capture problem as defined in the text. The algorithm used is developed and the computer implementation is described in detail in reference 2. The inputs to NEWPSI are the Cartesian coordinates and heading angles at the initial and final points and the turning radii for the initial and final turns. The outputs are the coordinates of the end of the initial turn and beginning of the final turn, the heading of the straight segment between the turns, and the angles and arc lengths turned through.

The fixed horizontal path is treated as a sequence of degenerate capture problems. Subroutine TWOD calls NEWPSI to synthesize the horizontal track between successive pairs of waypoints starting at the final waypoint and working backward to the initial input waypoint. This operation is carried out only when the STOLAND system is first activated or when an input waypoint is altered.

The horizontal capture path is controlled by subroutine TST. TST uses the estimated wind profile, the current airspeed of the aircraft, the nominal airspeed at the capture waypoint, and a specified value of bank angle to determine the turning radii used in the synthesis; then the input variables are set to the appropriate values and NEWPSI is called. After each call to NEWPSI during the synthesis of either the fixed or capture horizontal path, the necessary input and output variables are stored as described in the following section on the speed-altitude profile synthesis.

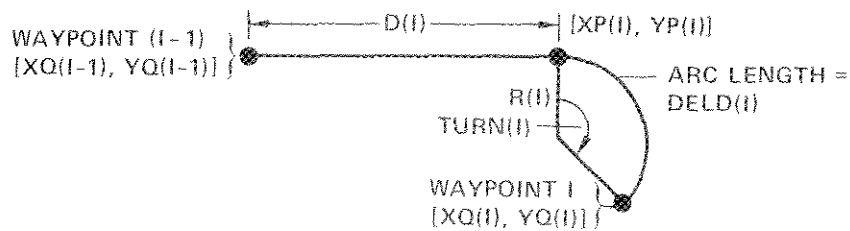
Speed-Altitude Profile Synthesis

The speed-altitude profile synthesis is carried out by three major subroutines, VHTSYN, INTEG, and STPINT, plus a number of auxiliary subroutines which will be discussed as needed. An explanation of the data structure is given first followed by a discussion of the operation of the major subroutines.

It is assumed that the horizontal path has already been synthesized as discussed earlier. The fixed portion is specified by NWP prestored waypoints, which are indicated on the pilot's display by a symbol and associated numbers from 1 through NWP. The pilot may select any of the fixed waypoints as the capture waypoint by entering the number associated with it through the keyboard. The actual waypoint numbers are greater by 2 than those on the display to allow waypoints 1 and 2 to be used for specifying the capture trajectory. Thus the capture waypoint number CURWPT is 2 greater than the number entered by the pilot. Waypoint 2 is defined as the end of the final turn in the capture trajectory and is therefore identical with the capture waypoint. Waypoint 1 is a special case and will be discussed later.

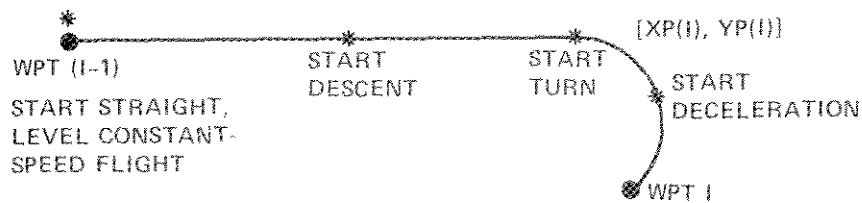
The total number of waypoints on the horizontal track is $(NWP + 2 - CURWPT)$. Note that the sequence of waypoint numbers is discontinuous at CURWPT. For

example, if CURWPT = 5 the sequence is 1, 2, 5, 6 . . . , NWP + 2. The horizontal track is specified by a set of column vectors each having one element per waypoint. These elements are defined according to the convention used in reference 7 as illustrated in sketch a. Associated with waypoint I is the straight line distance $D(I)$ from waypoint (I-1) to the point $XP(I), YP(I)$. That point is at the beginning of a turn (sketch a) through angle $TURN(I)$ with radius $R(I)$ terminating at the point $XQ(I), YQ(I)$, which is by definition the same as the waypoint coordinates, $XWP(I), YWP(I)$. The arc length of the turn is $DELD(I) = R(I) TURN(I)$, and $TURN(I)$ is positive clockwise. In addition to these quantities the nominal equivalent airspeed, $VA(I)$, and nominal altitude, $-ZWP(I)$, at each waypoint are needed for the profile synthesis. Note that the (X, Y) coordinates are not used in the profile synthesis but are needed to generate the complete trajectory in real time, and that the capture waypoint and $XQ(2), YQ(2)$ are the same point.

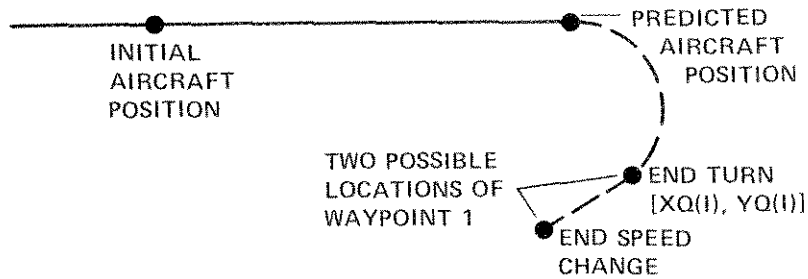


Sketch a.

Between waypoints (I-1) and I, speed and altitude changes may be initiated in addition to the turn, as shown in sketch b. These points, indicated by asterisks in the sketch, where changes in speed, altitude or heading are initiated, are referred to as command points. The waypoint is also a command point, and thus there will be from one to four command points for each waypoint. The special case of waypoint I is illustrated in sketch c. The initial aircraft position is predicted ahead 15 sec, assuming straight, level constant-speed flight to $[XP(1), YP(1)]$ where the turn and speed change, if necessary, are initiated. The altitude is held constant. Waypoint I is located at the end of the turn or when the desired speed, V_{TA} , is attained, whichever comes last.

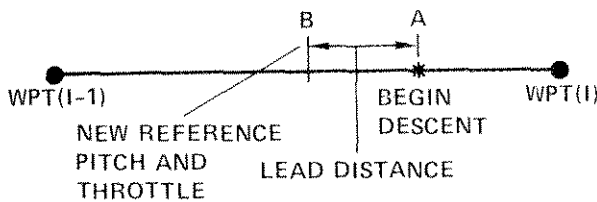


Sketch b.



Sketch c.

During the real-time forward generation of the profiles, the control of the aircraft to the reference trajectory can be improved by introducing impending changes in the reference controls some distance ahead of the command point as shown in sketch d. Here the reference trajectory begins to descend at point A; the new reference pitch and throttle commands will be introduced to the control system at point B, and the distance from A to B is referred to as the lead distance.



Sketch d.

The end product of the synthesis is a two-dimensional array, TCOM (IMAX,16) referred to as the command table, and three integer column vectors IWPTT, IVHT, and KCORT. The dimension of the column vectors is equal to the number of rows, IMAX, in TCOM, where

$$IMAX = 4(NWP - CURWPT + 2) ,$$

that is four times the number of waypoints, or one row for each command point. The various entries in the TCOM array will be explained subsequently.

VHTSYN acts as an executive for the profile synthesis, calling INTEG to synthesize the profiles between successive pairs of waypoints. INTEG in turn calls STPINT, which uses the energy-rate tables to compute the derivatives necessary for each integration step. The input variables for INTEG and the data loaded into them at waypoint I for integration forward to waypoint (I + 1) or backward to waypoint (I - 1) are summarized in table 2. Note that for I = 1 the values of ZWP(I), VA(I), and H(I) are those of the aircraft altitude, equivalent airspeed, and heading.

The output data from INTEG for each of the four command points are stored in a row of the transfer array TXFR, which has 16 columns whose elements are defined in table 3, and IXFR and KXFR, which are one-dimensional. Each row of TXFR is transferred into a row of TCOM. The transfer arrays are set to zero at the beginning of INTEG so that any unused rows will contain zero upon return to VHTSYN.

IVH and KCOR are flags, defined in the discussion of INTEG, which are stored in IXFR and KXFR, respectively. The flowchart in figure 12 illustrates

the operation of VHTSYN. First, the input data for waypoint 1 (the start of the first turn in the capture trajectory) are loaded according to table 2, and

INTBWS = 0

KSTOLS = 0

ALTO = ALTS

VIASN = V_{TA}

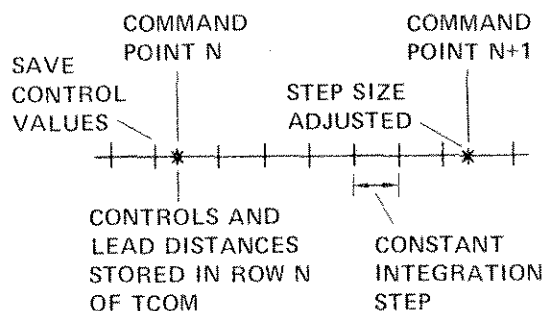
INTEG is called, and special logic in INTEG inserts into the first row of the transfer arrays the starting conditions for the straight constant-speed prediction of the aircraft motion ahead to provide time for the synthesis calculations. Then, the forward integration continues until the first turn has been completed and the desired speed achieved. Since for waypoint 1, there may be a segment of straight (changing speed) flight after the turn, that waypoint cannot be completely defined until the forward integration has been completed. The data from the forward integration are stored in the first four rows of TCOM, IXFR, and KXFR, the lead distances being shifted for compatibility with the results of the backward integration.

Next, the backward integration from the final waypoint (waypoint number NWP on the pilot's display and NWP + 2 in the computer) to waypoint 1 is initiated, and the data are stored in TCOM, IVHT, and KCORT from the bottom up. The waypoint number is stored in corresponding rows of IWPTT. The sign of the first column of TCOM (time) must be reversed in this case. If a complete synthesis has already been done, the integration starts at the capture waypoint. When waypoint 1 is reached, the altitude and speed are compared with the target values; if they are not equal an error return results. If there is no error, the first two columns are summed backward from the final waypoint [TCOM(I, 1) = TCOM(I, 1) + TCOM(I - 1, 1), etc.] to convert them to time and distance-to-go to the final waypoint. The lead distances in columns 13-16 are converted to distance-to-go by adding the corresponding values from column 2. Finally, other adjustments to the data are made to improve the reference control motions when the distances between command points are small.

It will be noted that since not every waypoint will have four command points, many of the rows of TCOM contain no useful data. However, the retention of this form makes it possible to resynthesize the profile backward in time, using a background computation, while the aircraft is flying along a reference trajectory being generated in real time from the results of the previous synthesis. This capability is desirable for adding time-control capability to the system.

INTEG synthesizes the speed-altitude profile between waypoints I and (I ± 1), where the plus-or-minus sign corresponds to forward or backward integration. The input and output variables for STPINT, the major subroutine called by INTEG, are defined in tables 4 and 5; table 6 defines a number of internal variables and flags that are of significance.

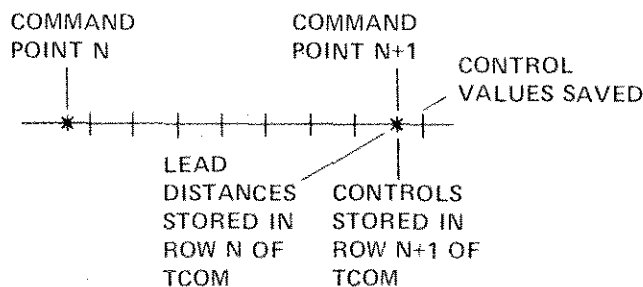
It must be remembered that the data stored at each command point are to be used to initialize the integration in the forward direction and to provide the lead distance needed to compensate for instantaneous changes in the controls at the command point. Sketch e illustrates the operation of INTEG in the forward direction.



Sketch e.

Between command points a fixed time interval is used as the integration step, except for the last step in the segment, which is adjusted to give the exact distance to the next command point. At each integration step, the bank angle is computed and then STPINT is called to compute the reference controls and the time derivatives of airspeed and altitude. These derivatives and the groundspeed are used in a rectangular integration to increment airspeed, altitude, and along-track distance. Just prior to command point N the values of the controls ϕ , π , δ_f , and v are saved, for example, $\phi_z = \phi$. At the command point the parameters controlling the type of flight are changed and STPINT is called. The new and saved control values are used to compute the lead distances.

For backward integration, the order of storing the controls and computing lead distances is reversed, as shown in sketch f. This means that for the new controls stored in row N + 1 of TCOM the lead distances are stored in row N. Note that in VHVSYN the lead distances computed in the forward integration are shifted up one row in TCOM to correspond to the results from backward integration.



Sketch f.

The preceding discussion dealt with the transition between two command points whose locations were assumed for simplicity to be known. The complete synthesis between two waypoints, including the location of the command points, is explained for the backward integration using figure 13. The case illustrated requires a turn as well as changes in speed and heading. After each call to STPINT the resulting changes in speed, altitude, and distance are tested to see whether the target values of speed, altitude, heading (expressed as arc length), or distance (the next waypoint) will be accomplished within the next integration step. If such is the case, the integration step is adjusted to the exact length required and the variables are stored in the

transfer arrays. If a speed or altitude change has been completed, the value of speed or altitude stored is set equal to the target value. Similarly, the distance at the end of a turn or the end of a waypoint is also set to the target value. This procedure eliminates such numerical errors as may arise during the integration.

The forward integration operates in essentially the same manner except for some special logic to account for the path between the aircraft and its predicted position discussed earlier.

If the integer KSTOLS is set to zero the minimum value of \dot{E}_n is constrained (in STPINT) to its value on the 84%-power contour. During the synthesis of the profiles between two waypoints, if the final speed for forward integration or initial speed for backward integration is greater than VIASTS (defined as the speed at which the 5.6°-flap and 84%-power contours intersect), KSTOLS is set to zero. The integer KNTRJ is set to zero during synthesis, causing the calculation of the angle of attack in STPINT to be bypassed in order to reduce computation time.

The variables DALT and DEV are the energy changes between the two waypoints due to change in altitude and airspeed, respectively. If they are of the same sign, VADTG and SINGAM are computed in STPINT to have the maximum magnitudes consistent with the various limits. If DALT and DEV are of opposite sign, one of them must exceed, in magnitude, the total energy change DEE, and a transfer between kinetic and potential energy is required. If $|\text{DEV}| > |\text{DALT}|$ then VADTG is set to its maximum allowable magnitude and SINGAM is chosen so that the changes in altitude and speed take place in the same time interval. CEPS is set to DALT/DEV; SINGAM, VADTG, and \dot{E}_n will be held constant in STPINT.

STPINT uses the energy-rate tables to compute the derivatives and control settings to be used in INTEG. In order to explain the interpolation process it is useful to assume that each of the data storage points, indicated by circles in figure 1, represents an element (i, j) in a 6×7 array. There are six of these arrays, one each for equivalent airspeed, normalized energy rate, angle of attack, nozzle angle, power setting, and flap deflection. The arrays of the first three quantities plus a 4×1 array of nozzle angles are stored for each of the four combinations of weight and altitude. The elements of the remaining three arrays are known implicitly from the data structure, as shown in figure 14. Note that the arrays in the figure are simply a device used for explanation; they are not actual sets of stored data. The first four rows of the power-setting array in figure 14(a) are constant-power contours, and the last two rows call for the minimum allowable power. The maximum allowable power, THMAX, is a function of temperature and must be computed as needed. Figure 14(b) shows the required flap settings. The quantity F_1 is defined as the minimum of the placard setting, or 65° , and F_2 is the minimum of the placard setting, or 45° . The nozzle angle shown in figure 5(c) is at its minimum value except for column 1, rows 1 through 4, and row 5, columns 1 through 4, which are set to stored values; and row 6, which is at the maximum value of 100° .

The first operation carried out in STPINT is the linear interpolation of the airspeed array over weight and altitude. The interpolated array, TVAV, contains the seventh column, with all the elements set at 160 knots. The airspeed interpolation is carried out by calculating a set of interpolation coefficients, one for each flight condition. Then each element of the interpolated array is the sum of the four corresponding elements in the stored arrays, each multiplied by the appropriate coefficient. Note that by definition column 7 corresponds to the maximum equivalent airspeed of 160 knots, so that only the first six columns of the four airspeed arrays are stored. The 4×1 nozzle array is also interpolated in this operation.

Once the interpolated airspeed array has been calculated it is used to carry out a simultaneous interpolation with respect to airspeed, weight, and altitude for the other five variables of interest. This interpolation proceeds one row at a time as follows: first the row is searched to find the airspeeds bracketing the current value, and two airspeed interpolation coefficients are calculated. Next, the elements of the flap, throttle, and nozzle arrays corresponding to the bracketing speeds are calculated and interpolated with respect to speed. This procedure is equivalent to drawing a vertical line on the energy-rate diagram and finding the values of the variables at the points of intersection with the horizontal contours defined by the rows of the arrays in figure 4. The constant flap contours described by columns 2 through 5 in figure 5(b) are not vertical, so that the constant airspeed line may also intersect them. These intersections are located by searching the columns for bracketing airspeeds in adjacent rows, and using linear interpolation as before. The values of E_n and α for the bracketing speeds are interpolated over weight and altitude using the coefficients computed earlier and then over speed. The results of this operation are interpolated values of E_n , v_s , δ_f , π , and α , stored in the columns of the $5 \times n$ array, TCV, which will have from three to nine rows, depending on the flight condition. For example, if a vertical line is drawn at the 70-knot point in figure 1, only 3 rows of data would be stored in TCV corresponding to the intersection of the vertical line with the control contours.

The average computation time required for one pass through STPINT on the airborne computer is 20 msec. This indicates that a major portion of the computation time for both synthesis and real-time reference generation is used in this subroutine.

The remainder of STPINT determines the output values EDTVA, SINGAM, and VADTG (of E_n , $\sin \gamma_a$, and \dot{V}_a , respectively) and the associated control in conformance with the inputs and constraints. The significant operations performed are itemized below:

1. If the estimated ambient temperature is greater than that used in computing the energy-rate tables, limit EDTVA so that $\pi(\text{EDTVA}_{\text{max}}) \leq \pi_{\text{max}} * \text{RTCFCFE}$
2. Correct limits on EDTVA for wind shear and bank angle
3. Set limits on EDTVA to use only positive or only negative values

- 4a. $EDTVA = RR \cdot (EDTVA_{\max} \text{ or } EDTVA_{\min})$ unless $CEPS \neq 0$
- 4b. $CEPS \neq 0$ (speed and altitude changing in opposite directions), in which case $EDTVA$ is computed from input $VADTG$ and $SINGAM$
5. If $\delta_f > 30^\circ$, limit $|VADTG| \leq 0.05$
6. If $KSTOL = 0$, limit $EDTVA \geq \dot{E}_n$ on 84%-power contour
7. If $EDTVA$ exceeds limits, adjust RR and start over at (1)
8. If $VADTG$ or $SINGAM$ exceeds limits, adjust EPS and return to (1)
9. Compute controls from TCV array using linear interpolation
10. RETURN

Real-Time Reference Trajectory Generation

To fly the aircraft along the reference trajectory, the reference states must be generated in real-time in the forward direction at time intervals small enough (0.1 sec was used) for proper functioning of the perturbation control system. The computations are done, as stated earlier, partly in far background and partly in foreground. Subroutine $NOMTRJ$ generates the set of variables defined in table 7 and stores them for later use in foreground by subroutine $NOMTR2$.

$NOMTRJ$ computes the same reference states and controls computed by $INTEG$ during the syntheses by performing the same operations as in $INTEG$. In this case, however, the integration always proceeds forward in time, and the type of flight and length of segments between command points are determined from the command tables. The integration step sizes are 1 sec during speed changes and 2 sec at all other times. The step sizes used in $NOMTRJ$ and $INTEG$ differ only in that the latter uses a single step to cover segments of straight, level, and constant-speed flight. When the track mode is engaged, the variables in $NOMTRJ$ are initialized to the values in the first row of $TCOM$. $STPINT$ is called and all of the variables except DNM defined in table 7 are stored (in the same order as shown in table 7) in the first column of a 15×6 array, $RDERIV$. Then the integration is carried forward one step and DNM is decreased by the distance covered in the integration step and stored in $RDERIV$. As the integration proceeds, the variables at the beginning of each integration step are stored in $RDERIV$ in this fashion. At the end of a segment between command points, the step size is adjusted to the exact value required to reach the command point. When data at a command point are stored in a column of $RDERIV$, the corresponding element of the 6×1 array $KDERIV$ is set to 1, otherwise it is set to zero.

$NOMTR2$ uses distance along the reference horizontal path as the independent variable and computes the reference time, ground heading, airspeed, and Cartesian components of position and ground velocity. The speed, heading, and

components of position are initialized at those of the aircraft at the beginning of the synthesis (that is, at P_1 in fig. 10). The remaining variables are initialized at the values in the first column in RDERIV. The computation of the reference states then proceeds, using a step size roughly equivalent to 0.1 sec. The integration step size, as discussed earlier, is nominally the along-track distance between the reference position and the aircraft position as determined by the navigation system. At the beginning of the reference trajectory computation the first integration step size will therefore be equal to the along-track-distance covered during the synthesis computations. The restrictions on the rate of change of reference position mentioned earlier are not applied in this case and the changes in reference time and the reference states due to travel along the predicted flightpath during the synthesis computations are accounted for. The integration in NOMTR2 then proceeds, using a step size corresponding roughly to 0.1 sec, under the assumption that all of the variables in table 7, except the speeds, remain constant. When the next integration step would move the reference position beyond the next point for which data are stored in RDERIV, the step size is set to the exact value needed to reach that point. Then the variables are set to the values in RDERIV. If the corresponding element of KDERIV is nonzero, indicating a command point, the reference altitude, airspeed, and time are set to the values in the new row of TCOM; if KCOR indicates the beginning or end of a turn or a new waypoint, the X and Y coordinates, heading angle, and turning radius are reset to the appropriate values from the arrays defined in the section on the speed-altitude profile synthesis. This correction process has been generally successful in keeping computation errors small.

The intersection between NOMTRJ and NOMTR2 is best understood with the aid of the simplified flowchart shown in figure 12. After each integration step in NOMTRJ the variables are stored in a column of RDERIV and the computations are carried out so that the variables are stored for several seconds ahead of current time. As the real-time integration in NOMTR2 proceeds from one column of RDERIV to the next, new values must be computed by NOMTRJ to replace the old values that have been used. The logic for this procedure is as follows: the number of the column to be computed next is IC, and IU is the number of the column to be used next. The integer KINT is nonzero if there are no columns in RDERIV to be computed, in which case NOMTRJ is bypassed. Initially $KINT = 0$ and $IC = IU = 1$. The first column of RDERIV is computed and IC is set to 2. Next, the first column of RDERIV is used and a 0.1-sec integration step is made. If the point corresponding to the next column of RDERIV is not reached, IU does not change. The integer IDL denotes the number of columns of RDERIV that contain data usable in the future. The logic operates to maintain $2 \leq IDL \leq 5$. If as a result of insufficient background time $IDL = 0$, an error return results. However, this situation has not been encountered in flight or in simulation tests.

Foreground Computation

A portion of the foreground computation was discussed in the section on real-time trajectory generation. Most of the remainder of the foreground computation is done in subroutine CNTRL. The variables of interest are listed

in table 8. The operation of the subroutine is explained with the aid of the simplified flowchart shown in figure 15. At the start of the real-time trajectory generation the error feedback quantities are initialized at zero. The first operation performed in CNTRL is the computation of the speed and altitude errors, the flap command, roll command, and temporary values for the nozzle and throttle commands. The latter are the solutions of rows 1 and 3, respectively, in equation (31). The flap command is the smaller of the reference value and the placard value at the current airspeed obtained from the navigation system; the roll command is given by equation (27). Next the minimum value of the power setting, THL, including perturbation controls, is computed. For reference flap settings of 45° or more, $THL = \max(89.5\%, THACR - 2.0\%)$.

If the temporary power setting, THIMP, is less than THL it is set equal to THL, and PFT is the fraction of the desired perturbation from the reference power setting that is actually achieved, that is, $PFT = (THL - THIMP) / (THACR - THIMP)$. The temporary nozzle perturbation is multiplied by $(1 - PFT)$, that is, by the fraction of the desired change in power setting that is not achievable.

In the case in which the temporary power setting is greater than or equal to THL, PFT is set to zero, and the temporary nozzle command is usually less than the reference value. If the reference nozzle is 45° or greater, the temporary nozzle command is set to the greater of its computed value or 45°, but if the reference value is less than 45° the temporary nozzle command is set equal to the reference value. These restrictions are necessary to prevent violation of the maneuver margin.

Next, the nozzle and throttle commands are set equal to the temporary values and limited between the prescribed maximum and minimum values. The perturbation in pitch angle is computed from row 2 of equation (31) and multiplied by $(1 + 0.6 PFT)$. This multiplying factor and the values used for PFT are the result of the linearized analysis and simulation and flight tests.

After the control commands have been computed, a new set of aircraft states is obtained from the navigation system; this occurs regularly at 0.1-sec intervals. The integrals of the speed and altitude errors are incremented subject to limits on their magnitude. Experience dictated setting the limits on both error integrals at that value which would call for a change of 2% rpm in power setting. Next, the along-track position deviation, DXAT, and the crosstrack position, error, and error rate are computed, and the integration distance step DED to be used in NOMTR2 is set equal to DXAT. If KCOM = 1, indicating the initial straight, level constant-speed segment of flight at the beginning of the capture trajectory, DED is restricted to positive values. That is, if the aircraft is ahead of the reference position (the normal initial condition), the reference position is immediately advanced to the along-track aircraft position. If the aircraft is behind the reference position, the latter is held fixed until the aircraft catches up. After the first segment of the capture trajectory, DED is constrained to be within ±40% of the distance covered in 0.1 sec at the reference groundspeed. This restriction, as mentioned earlier, is used to prevent excessive control action due to

sudden large changes in the estimated aircraft states. In case of severe errors, this restriction allows large along-track errors to develop, and the pilots must be warned. Before CNTRL is entered again, NOMTR2 is called and the reference states are updated.

REFERENCES

1. Lee, Homer Q.; Neuman, Frank; and Hardy, Gordon, G.: 4D Area Navigation System Description and Flight Tests. NASA TN D-7874, 1975.
2. McLean, John D.: A New Algorithm for Horizontal Capture Trajectories. NASA TM-81186, Mar. 1980.
3. Erzberger, Heinz; and McLean, John D.: Fuel Conservative Guidance System for Powered-Lift Aircraft. AIAA Guidance and Control Conference, Boulder, Colorado; AIAA Paper 79-1709, Aug. 1979.
4. Flanagan, Paul F.: Implementation of an Optimum Profile Guidance System on STOLAND. NASA CR-152178, Sept. 1978.
5. Erzberger, Heinz; and Lee, Homer Q.: Constrained Optimum Trajectories with Specified Range. Journal of Guidance and Control, vol. 3, no. 1, Jan.-Feb. 1980.
6. Erzberger, Heinz; and Lee, Homer Q.: Terminal-Area Guidance Algorithms for Automated Air Traffic Control. NASA TN D-6773, Apr. 1972.
7. Pecsvaradi, Thomas: Four-Dimensional Guidance Algorithms for Aircraft in an Air Traffic Control Environment. NASA TN D-7829, Mar. 1975.
8. Jakob, Heinrich: An Engineering Optimization Method with Application to STOL Aircraft Approach and Landing Trajectories. NASA TN D-6978, Sept. 1972.
9. Slater, Gary: Analysis of Integral Controls in Linear Quadratic Regulator Design. AIAA Guidance and Control Conference, Boulder, Colorado; AIAA Paper 79-1743, Aug. 1979.

TABLE 1.- FLAGS USED IN FAR BACKGROUND COMPUTATIONS

Flag	Purpose
WPN	Keyboard input capture waypoint
WNDENT	Nonzero if estimated wind profile is to be computed
CPTCNG	Nonzero if estimated temperature profile is to be computed
IFIX	If zero, compute speed-altitude profile for entire trajectory; if nonzero, for capture only
NOCAP	Zero if valid speed-altitude profile has been found
NCAP	Index of display message giving reason for no capture (computation not finished, desired speed not attained, desired altitude not attained)
ENGAGE	Nonzero if in track mode
WAYCAL	Nonzero if 2D fixed path to be computed
CURWPT	Current waypoint number initially CURWPT = 2
REFF	Nonzero to activate trajectory synthesis
HORNAV	Nonzero value starts forward integration and engages servos for automatic controls. (REFF must be set nonzero first)

TABLE 2.- INPUT DATA FOR INTEG

Variable	Definition	Set Equal to
DS	Distance to next waypoint	DELD(I) + D(I)
ALTS	Initial altitude	-ZWP(I)
DELDS	Arc length	DELD(I)
VIASS	Initial equivalent airspeed	VA(I)
RADIUS	Turning radius	R(I)
HEADGO	Ground heading	H(I)
TTURN	Turn angle	TURN(I)
WS	(aircraft weight)/cos ϕ	WT/COSPHI
KSTOLS	STOL mode flag	0
INTBWS	0 for forward integration	
ENUZ	Previous values of controls	
PHLZ		
GAMZ		
FLZ		
ALTO	Altitude and speed	-ZWP(I \pm 1)
VIASN	At next waypoint	VA(I \pm 1)

TABLE 3.- OUTPUT DATA FROM INTEG STORED IN TXFR

Variable	Definition	Column of KXFR
TIME	Time to next command point	1
DIST	Distance to next command point	2
GAMMA	Flightpath angle	3
STURN	0 for no turn + 1.0 for right turn - 1.0 for left turn	4
EPSLIN	Input value of ϵ	5
THAC	Power setting	6
FAC	Flap setting	7
FNUAC	Nozzle angle	8
PHI	Bank angle	9
ALT	Altitude	10
DEE	Change in energy between waypoints	11
VIAS	Equivalent airspeed	12
DSPHI	Lead distance for roll command	13
DSFAC	Lead distance for flap command	14
DSGAM	Lead distance for pitch command	15
DSNU	Lead distance for nozzle command	16

TABLE 4.- INPUTS FOR STPINT

Variable	Definition
DEE	Energy change between waypoints
ALT	Altitude
CEPS	(See discussion)
COSPHI	Cosine of bank angle
EDTMAX	Upper limit on \dot{E}_n
EDTMIN	Lower limit on \dot{E}_n
EPS	Epsilon
RTCFC	Temperature correction factor
RR	$1 - \sigma$
SGMX	Upper limit on SINGAM, $\sin(\gamma_A)$
SGMN	Lower limit on SINGAM
VIAS	Equivalent airspeed
VT	True airspeed
VDGMN	Upper limit on \dot{V}_a/g
VDCMX	Lower limit on \dot{V}_a/g
AKW	Wind shear factor
KSTOL	0 flaps cannot extend
KNTRJ	0 angle of attack not computed

TABLE 5.- OUTPUT VARIABLES FROM STPINT

Variable	Definition
ALPHA	Angle of attack
ENUAC	Nozzle angle
FAC	Flap deflection
SINGAM	Sine of aerodynamic flightpath angle
THAC	Power setting
THMIN	Minimum power setting
VADTG	\dot{V}_a/g
VIASST	Equivalent airspeed at intersection of 5.6 flap and 84% power contours

TABLE 6.- INTERNAL FLAGS AND VARIABLES FOR INTEG

Flag	Definition
IVH	1. Changing speed and altitude 2. Changing speed 3. Changing altitude 4. Constant-speed, constant-altitude turn 5. Straight, level constant-speed flight
ITURN	-1.0 left turn 0 no turn +1.0 right turn
KCOR	1,8 end of turn or end of waypoint 4 beginning of turn or waypoint
INTBWS	0 forward integration 1 backward integration
ISEG	1 start of IVH = 5 in forward integration 2 end of IVH = 5 in backward integration
IEND	1 end of waypoint
ICOM	1 one fractional integration step to end of segment
NSTART	0 start new segment between command points
KSTART	0 initialize synthesis between waypoints
KBWD	0 computing predicted aircraft position
Variable	Definition
DALT	Change in altitude between waypoints
DEV	Change in energy due to speed change between waypoints
VIASS	Equivalent airspeed
VTS	True airspeed
RAD	RADIUS * STURN
GAM	Aerodynamic flightpath angle
GAMMS	Inertial flightpath angle
CEPS	Nonzero for DALT and DEV of opposite sign
RATIOS	(true airspeed)/(equivalent airspeed)
VIS	Inertial velocity
VSG	Groundspeed
VTASN	Target true airspeed
RQ	Input value of RR

TABLE 7.- OUTPUT VARIABLES FROM NOMTRJ

Variable	Definition
DNM	Distance to final waypoint
VIASR	Equivalent airspeed
VADT	True airspeed rate
ALPHA	Angle of attack
ENUAC	Nozzle angle
FAC	Flap deflection
THAC*RTCFR	Power setting corrected for temperature
THMIN*RTCFR	Minimum power setting corrected for temperature
VWAT	Along-track component of wind
WKF	Used in fuel calculation
RTHET2	Used in fuel calculation
SINGMI/COSGMI	Tangent of inertial flightpath angle
RATIOR	Ratio of true to equivalent airspeed
VGNM	Groundspeed
PHID	Bank angle

TABLE 8.- VARIABLES USED IN SUBROUTINE CNTRL

Input Variables	Definition
XA, YA	Aircraft position coordinates
ALTA	Aircraft altitude
VIASA	Aircraft equivalent airspeed
GAMMA	Aircraft aerodynamic flightpath angle
XR, YR	Reference position coordinates
ALTR	Reference altitude
VIASR	Reference equivalent airspeed
GAMMR	Reference inertial flightpath angle
HR	Reference heading
FACR	Reference flaps
ENVACR	Reference nozzle angle
THACR	Reference power setting
PHIR	Reference bank angle
ALPHR	Reference angle of attack
KCOMR	Command table index
THMNR	Minimum reference power setting
Output Variables	Definition
FACC	Flap command
ENUACC	Nozzle command
THACL	Power command
PHIC	Bank angle command
THQC	Pitch command
DED	Integration step for NOMTR2
Internal Variables	Definition
DALT	Altitude error
DVEL	Airspeed error
DXAT	Along-track deviation between actual and reference position
DYCT	Crosstrack position error
DYDCT	Crosstrack error rate
THCTMP	Temporary power command
ENUTMP	Temporary nozzle command
THL1	$\text{MAX}(89.5, 7\text{HACR}-2.0)$
THL2	$\text{THACR}(\text{FACR}/45.0) + \text{THMNR}(1.0 - \text{FACR}/\text{er}.0) - \text{MIN}(0, -0.275 \text{DVEL})$
PFT2	$(\text{THL}-7\text{HCTMP}) / (\text{THACR}-\text{THC7MP}+.01)$
ENU1	$\text{ENVACR}-\text{PFT}(\text{ENUACR}-\text{ENUTMP})$

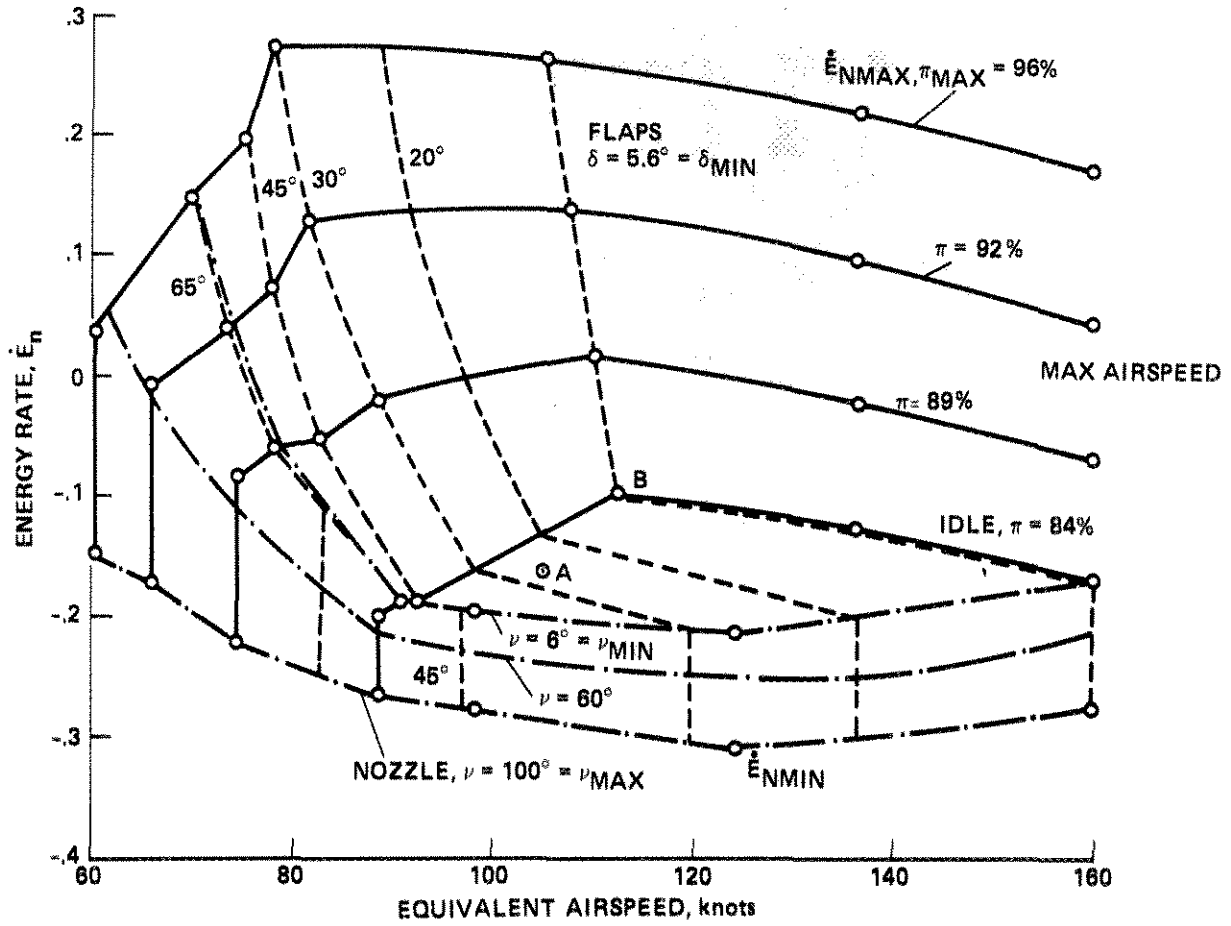


Figure 1.- Energy rate diagram for STOL aircraft; W = 38,000 lb, sea level 59° F.

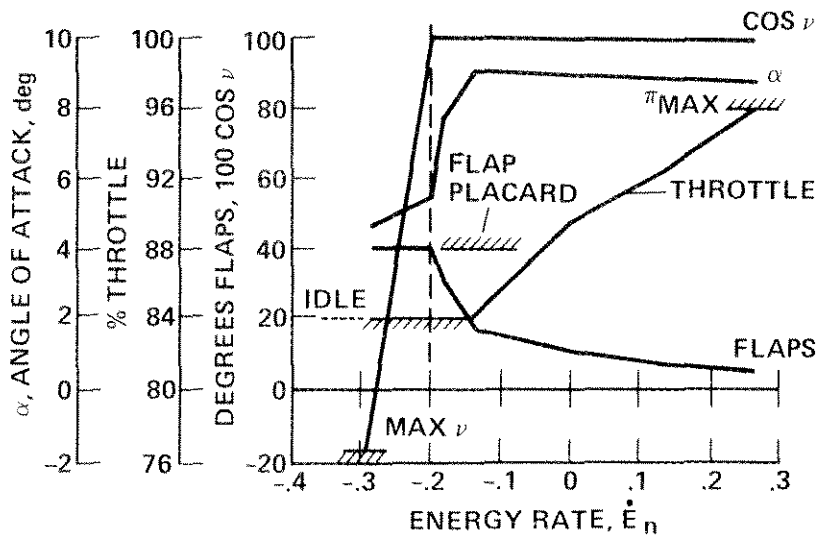


Figure 2.- Optimum controls as function of energy rate at 105 knots;
 $W = 38,000$ lb, sea level 59° F.

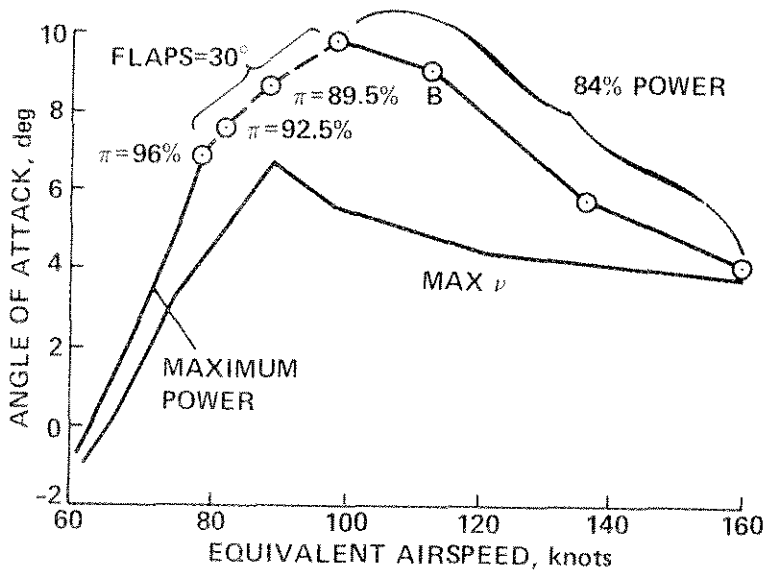
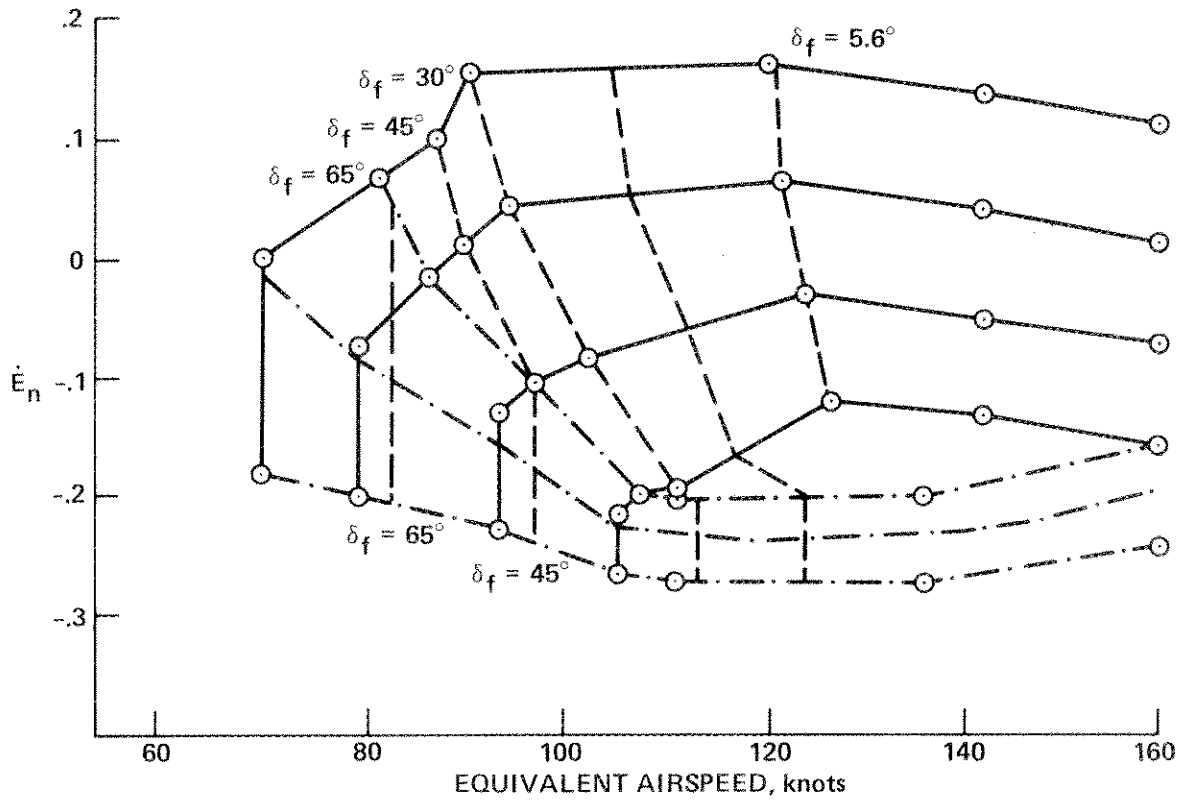
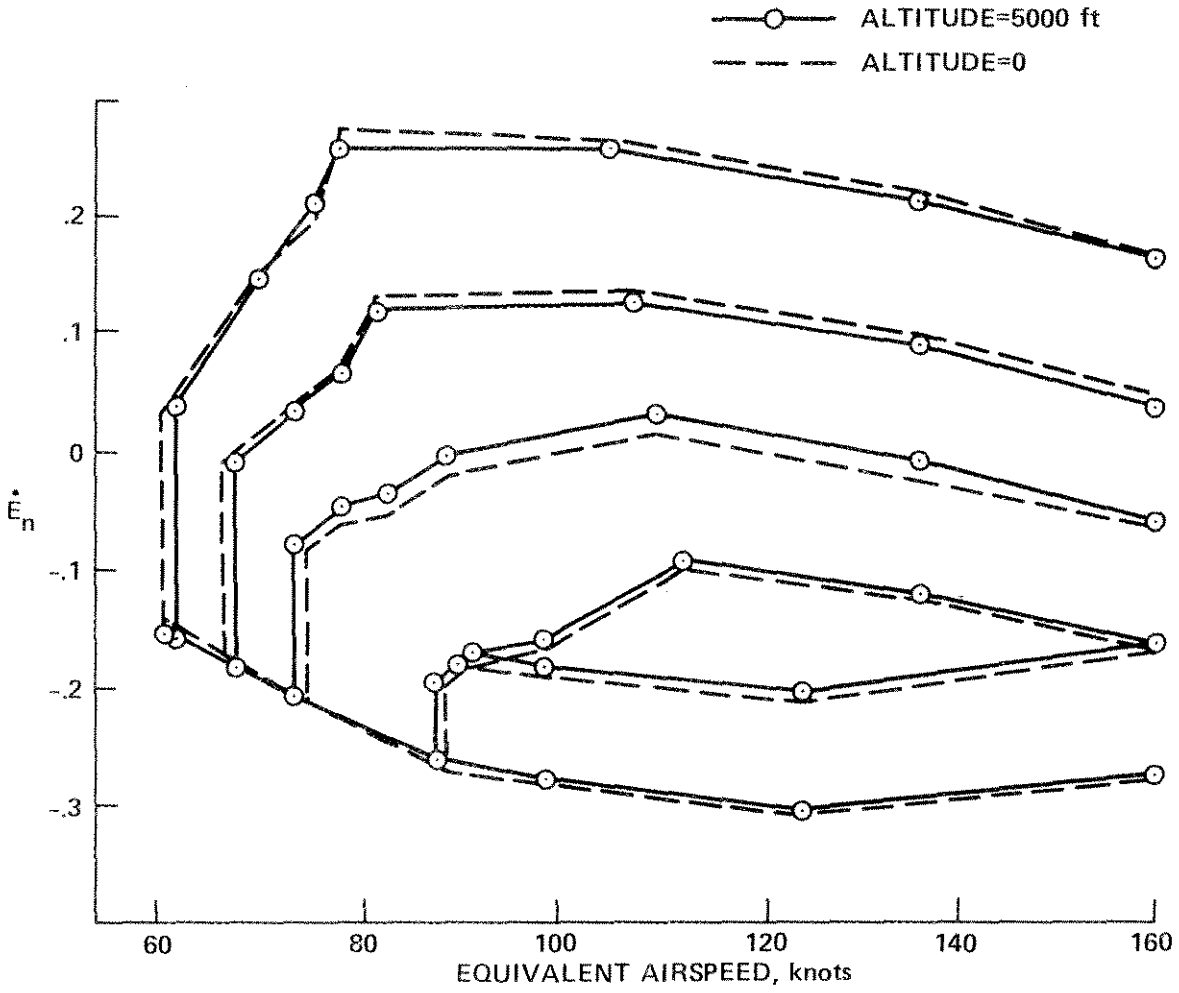


Figure 3.- Angle of attack for STOL aircraft energy-rate diagram.



(a) Energy-rate diagram for weight = 48,000 lb, altitude = 0.

Figure 4.- Energy-rate diagrams.



(b) Effect of altitude on energy-rate tables; weight = 38,000 lb.

Figure 4.- Concluded.

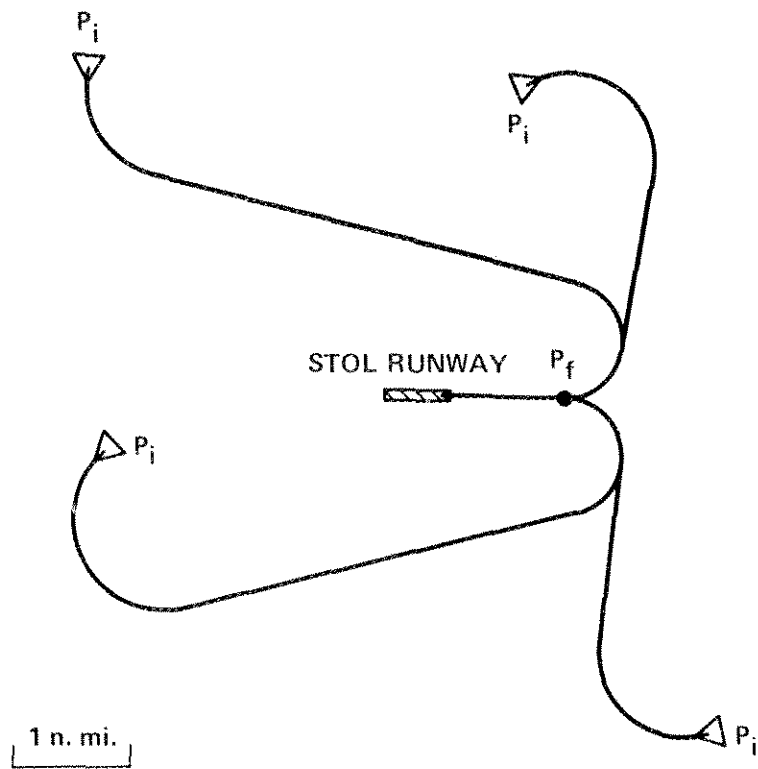


Figure 5.- Examples of minimum distance, constant turn radius, horizontal capture trajectories to a capture point P_f on final approach.

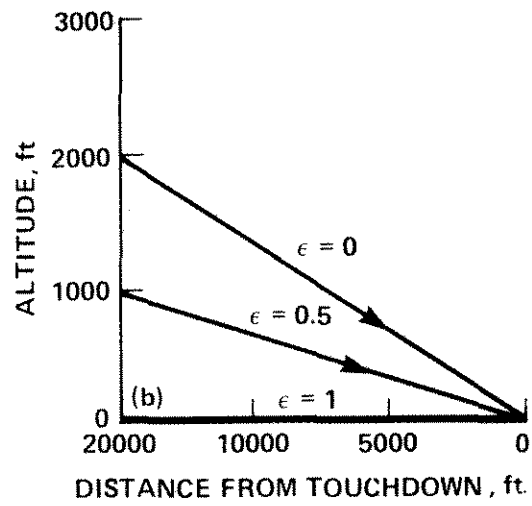
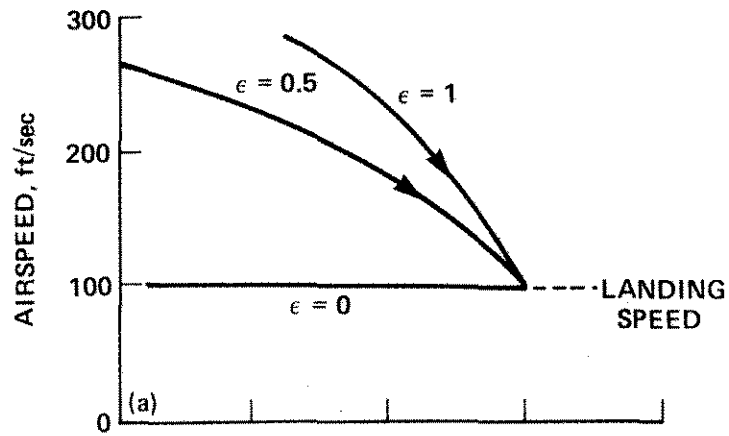


Figure 6.- Effect of ϵ on speed and altitude profiles, with $\dot{E}_n = -0.13$.

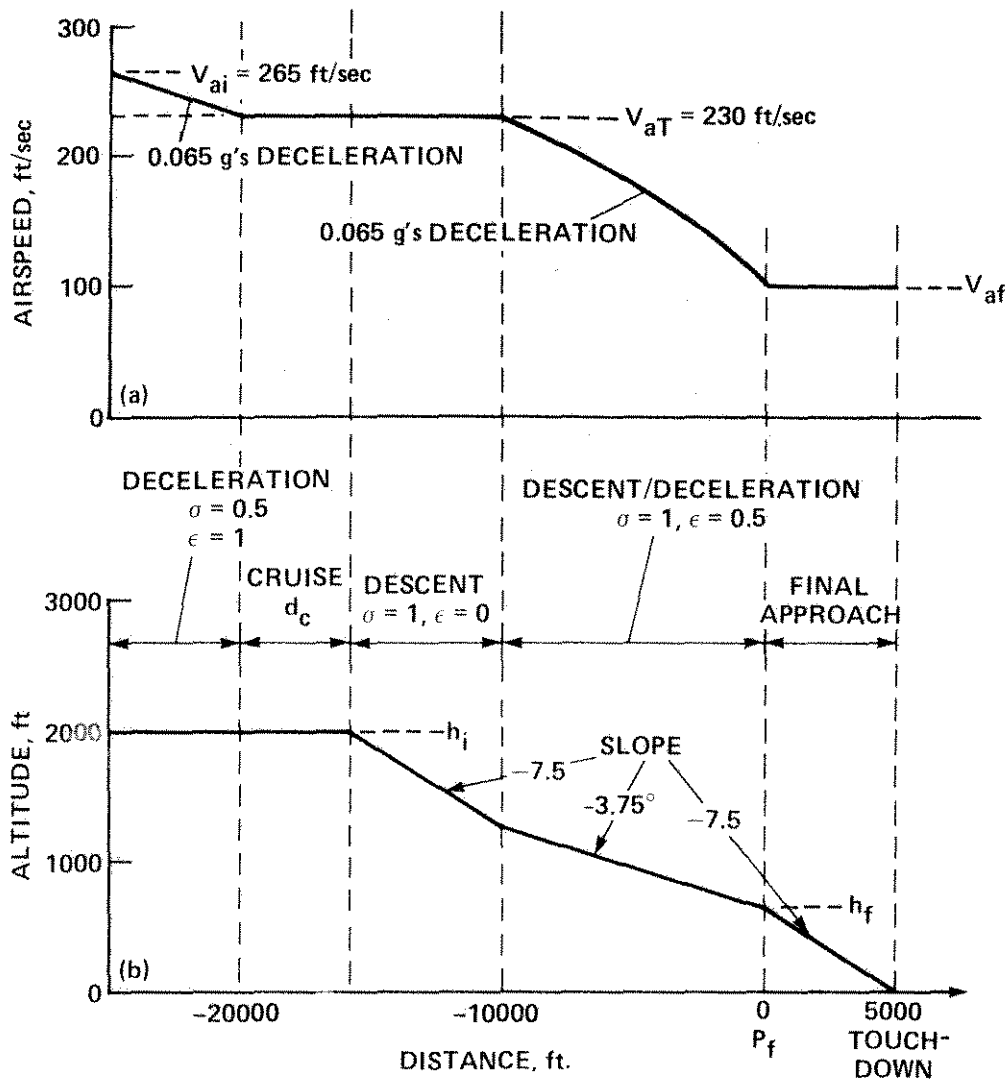


Figure 7.- Example of synthesized STOL approach trajectory.

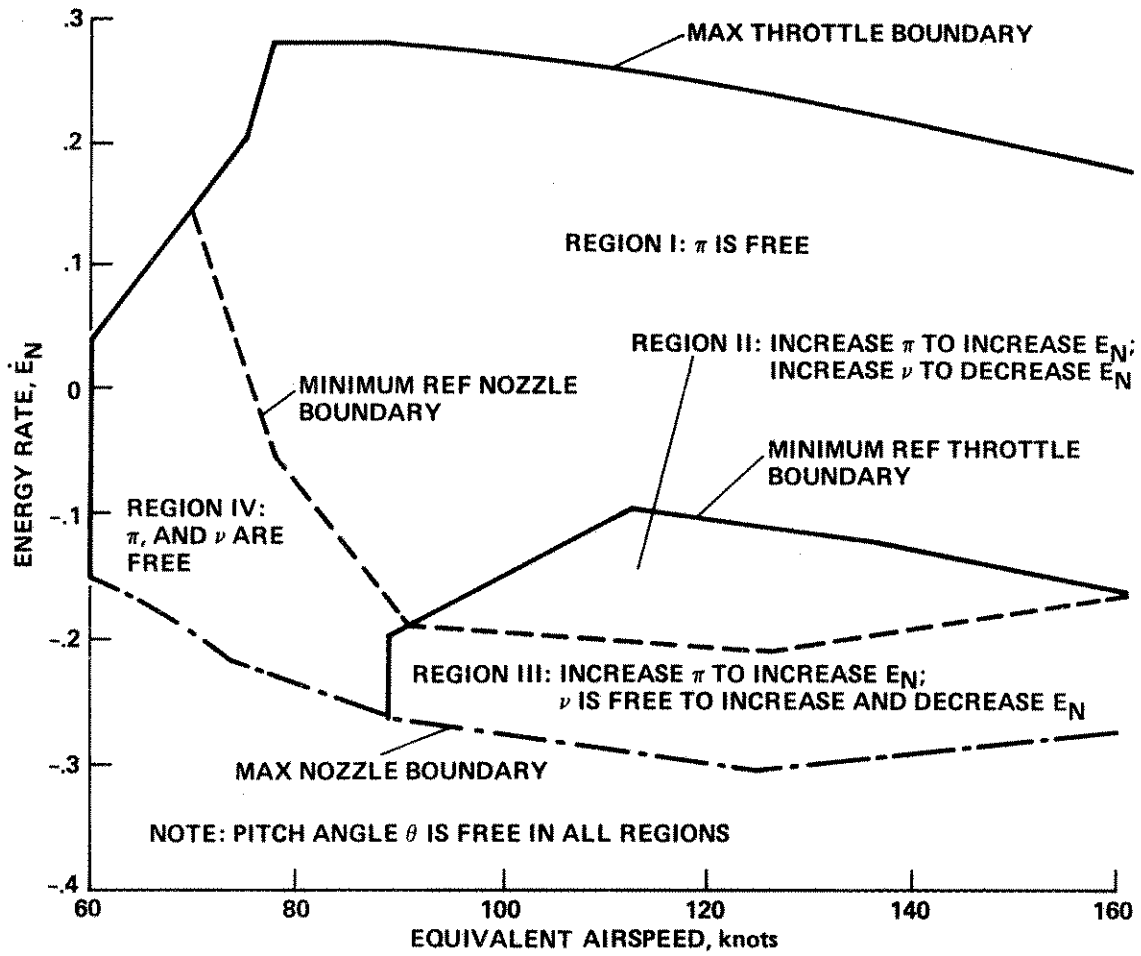


Figure 8.- Constraint boundaries for perturbation controls.

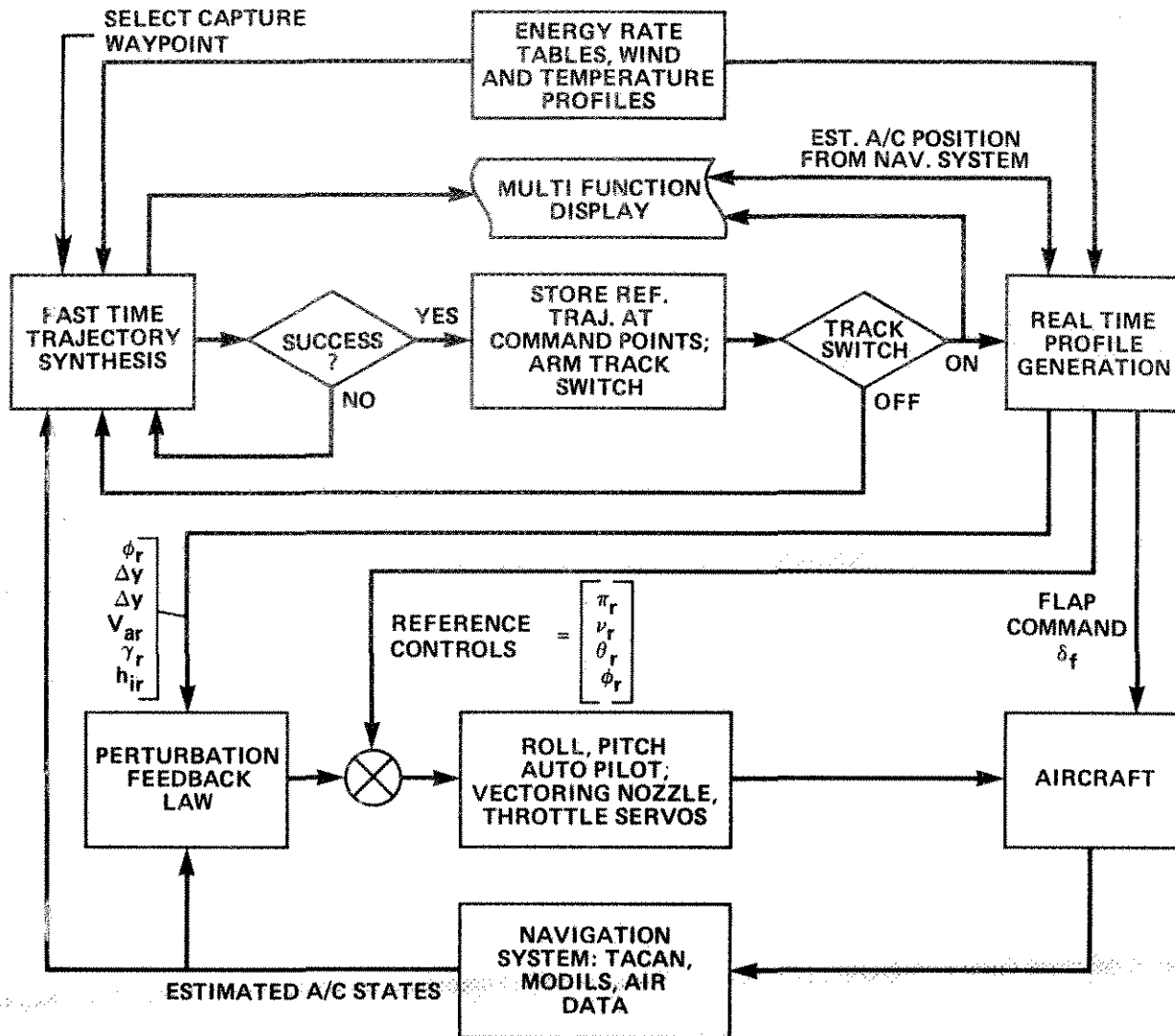


Figure 9.- Block diagram of guidance system.

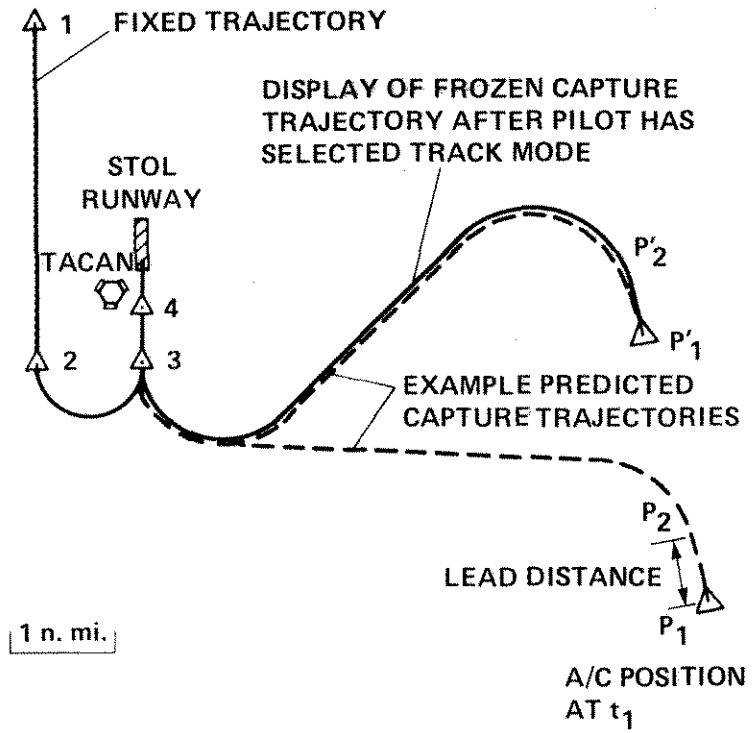


Figure 10.- Horizontal flightpaths displayed on cockpit Horizontal Map Display (HMD).

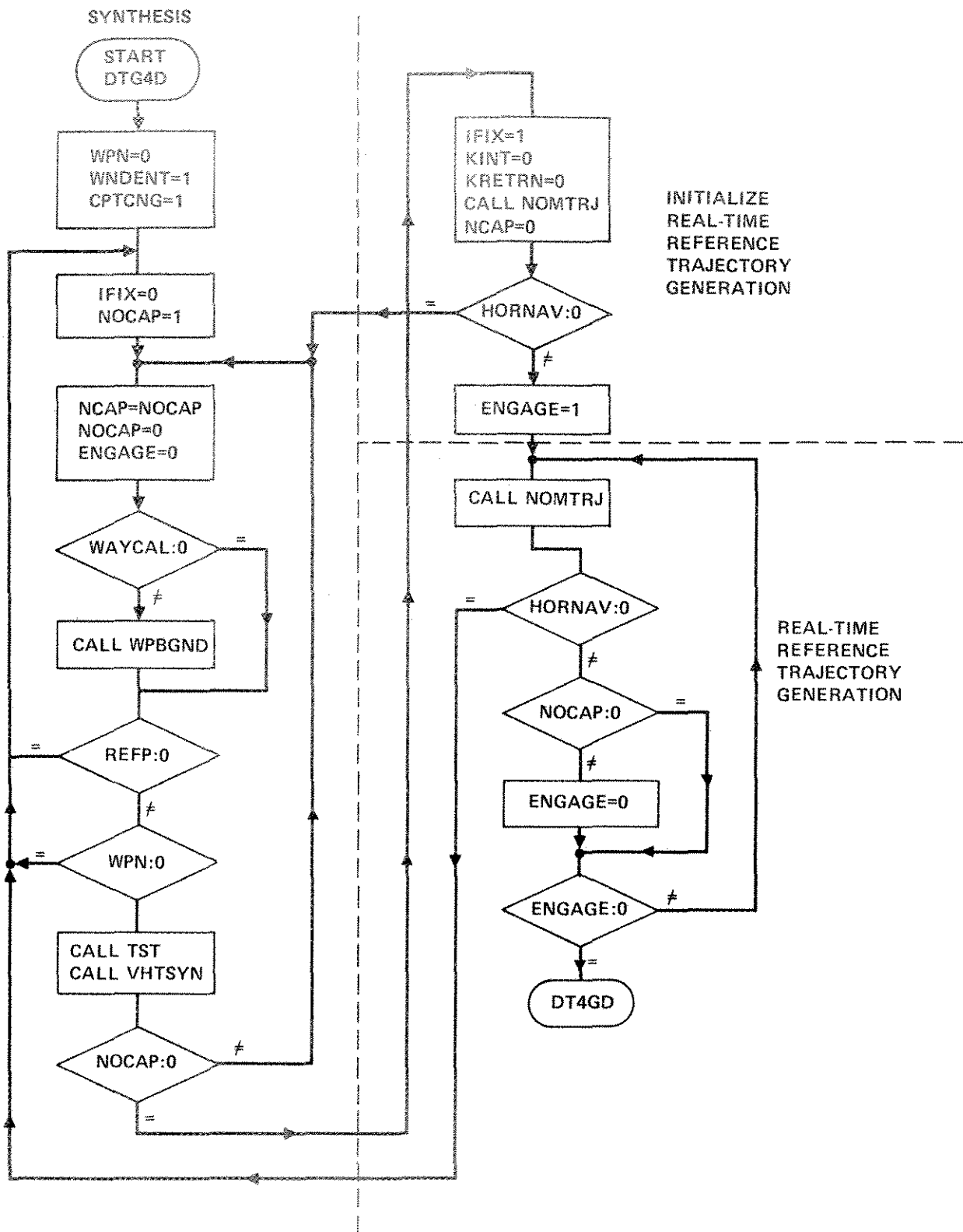


Figure 11.- Flow chart of background executive, D7G4D.

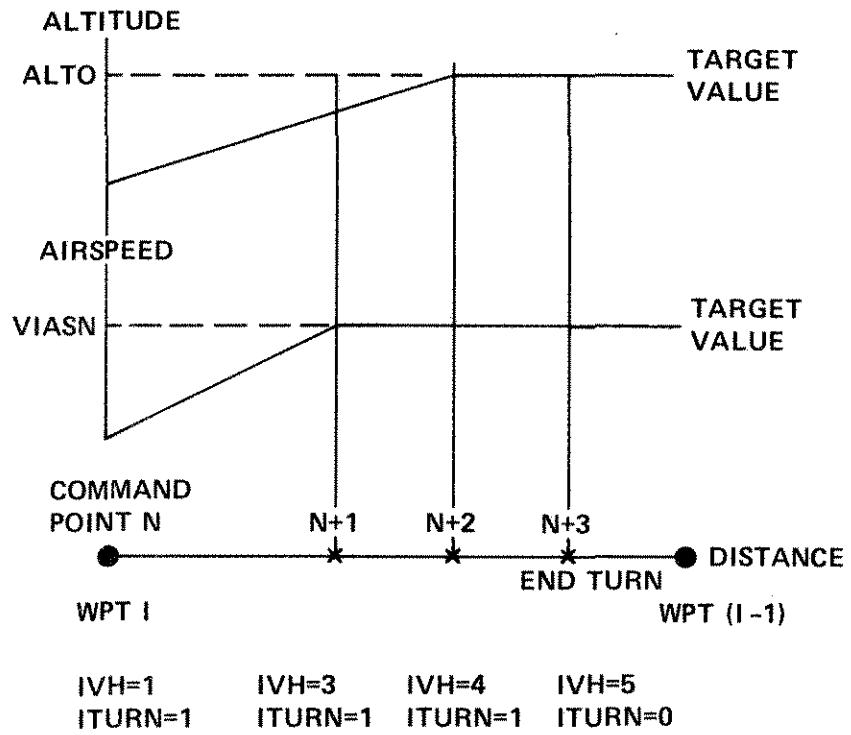


Figure 13.- Backward integration for speed-altitude profile synthesis.

COL ROW	1	2	3	4	5	6	7
1	THMAX						→
2	92.5%						→
3	89.5%						→
4	84.0%						→
5	THMAX	92.5	89.5	84.0			→
6	↓	92.5	89.5	84.0			→

THMAX = MAX
POWER SETTING

(a) POWER SETTING

COL ROW	1	2	3	4	5	6	7
1	F_1	F_1	45°	30°	5.6°	5.6°	5.6°
2	F_1	F_1	↓	↓	↓	↓	↓
3	F_2	F_2					
4	F_2	F_2	↓	↓	↓	↓	↓
5	F_1	F_1	F_2				→
6	F_1	F_1	F_2				→

F_1 = MINIMUM OF
65° OR PLACARD

F_2 = MINIMUM OF
45° OR PLACARD

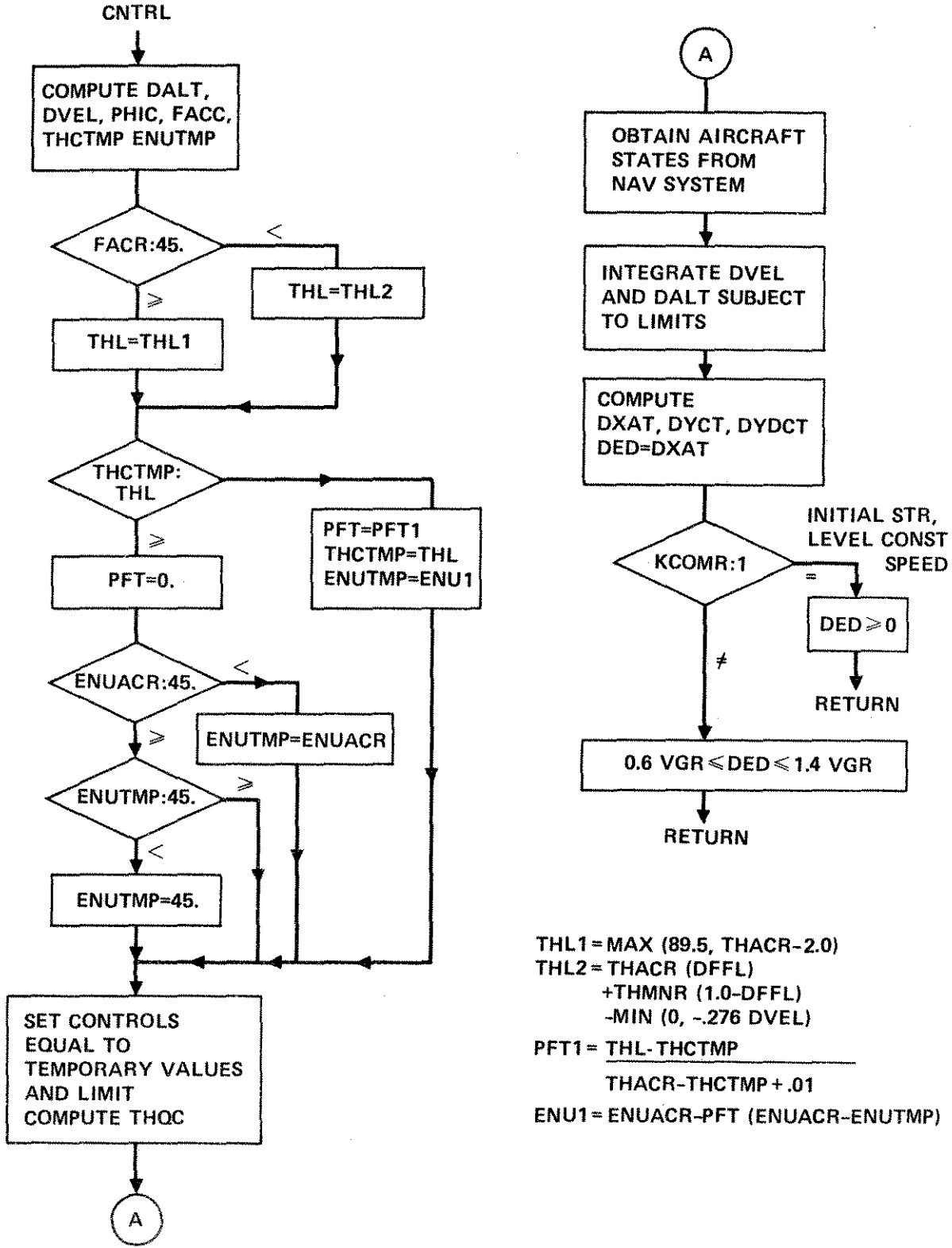
(b) FLAPS

COL ROW	1	2	3	4	5	6	7
1	N_1	6°					→
2	N_2	6°					→
3	N_3	6°					→
4	N_4	6°					→
5	N_1	N_2	N_3	N_4	6°		→
6	100°						→

N_1, N_2, N_3, N_4
ARE INTERPOLATED
VALUES OF STORED
DATA

(c) NOZZLE ANGLE

Figure 14.- Conceptual arrays of control values.



$THL1 = \text{MAX}(89.5, THACR - 2.0)$
 $THL2 = THACR(DFFL) + THMNR(1.0 - DFFL) - \text{MIN}(0, -.276 DVEL)$
 $PFT1 = \frac{THL - THCTMP}{THACR - THCTMP + .01}$
 $ENU1 = ENUACR - PFT(ENUACR - ENUTMP)$

Figure 15.- Flow chart of CNTRL.

1. Report No. NASA TM-81256	2. Government Accession No.	3. Recipient's Catalog No.	
4. Title and Subtitle DESIGN OF A FUEL-EFFICIENT GUIDANCE SYSTEM FOR A STOL AIRCRAFT		5. Report Date	
		6. Performing Organization Code	
7. Author(s) John D. McLean and Heinz Erzberger		8. Performing Organization Report No. A-8427	
		10. Work Unit No. 505-34-11	
9. Performing Organization Name and Address Ames Research Center, NASA Moffett Field, CA 94035		11. Contract or Grant No.	
		13. Type of Report and Period Covered Technical Memorandum	
12. Sponsoring Agency Name and Address National Aeronautics and Space Administration Washington, D.C. 20435		14. Sponsoring Agency Code	
		15. Supplementary Notes	
16. Abstract A fuel-conservative guidance system for powered-lift STOL aircraft operating in terminal areas has been developed and evaluated in flight. In the predictive mode, the system synthesizes a horizontal path from an initial aircraft position and heading to a desired final position and heading and then synthesizes a fuel-efficient speed-altitude profile along the path. In the track mode, the synthesized trajectory is reconstructed and tracked automatically. This paper presents an analytical basis for the design of the system and a description of the airborne computer implementation. A detailed discussion of the software, which should be helpful to those who use the actual software developed for these tests, is also provided.			
17. Key Words (Suggested by Author(s)) Aircraft trajectories Aircraft guidance Optimum trajectories Terminal area guidance		18. Distribution Statement Unlimited STAR category - 01	
19. Security Classif. (of this report) Unclassified	20. Security Classif. (of this page) Unclassified	21. No. of Pages 65	22. Price* \$8.00